Marine Geology 329–331 (2012) 75–92

Contents lists available at SciVerse ScienceDirect

Marine Geology

journal homepage: www.elsevier.com/locate/margeo

# The paleo-Etel River incised valley on the Southern Brittany inner shelf (Atlantic coast, France): Preservation of Holocene transgression within the remnant of a middle Pleistocene incision?

Guilhem Estournès [a,b,*], David Menier [a,c], François Guillocheau [d], Pascal Le Roy [e], Fabien Paquet [f], Evelyne Goubert [a]

[a] GMGL,UMR 6538 CNRS Domaines Océaniques, Université de Bretagne Sud, Centre de recherche Yves Coppens, Campus de Thoannic, 56017 Vannes cedex, France
[b] Lafarge Granulat Ouest, 9 Rue de la Motte, 35770 Vern-sur-seiche, France
[c] Universiti Tecknologi Petronas, Faculty of Geosciences and Petroleum Engineering, Bandar Seri Iskandar, 31750 Tronoh, Perak, Malaysia
[d] Géosciences Rennes, UMR 6118 CNRS, Université de Rennes 1, Campus de Beaulieu, Bat.15 35042 Rennes Cedex, France
[e] Institut Universitaire Européen de la Mer, UMR 6538 Domaines Océaniques, Technopôle Brest-Iroise, Place N. Copernic, 29280 Plouzané, France
[f] BRGM, GEO/GBS: Géologie des Bassins Sédimentaires, Bâtiment C1, 2ème étage, bureau 216, 3 av. Guillemin BP 36009-45060 Orleans cedex 2, France

ARTICLE INFO

*Article history:*
Received 3 February 2011
Received in revised form 16 August 2012
Accepted 17 August 2012
Available online 30 August 2012

Communicated by: J.T. Wells

*Keywords:*
incised valley
high resolution seismic
inner shelf
Southern Brittany
Pleistocene

ABSTRACT

The study of a dense and regular grid of 59 High Resolution seismic profiles supplemented by 23 superficial vibro-cores has led to propose a three-dimensional detailed sedimentary model of the paleo-Etel River buried valley located on the inner shelf of South Brittany (Atlantic Coast, France).
This fluvial valley (S2) lies at a mean depth of −37 m below mean sea level above Paleozoic meta-sediments (U1) and middle to late Eocene formations (U2). No fluvial deposits seem to have been preserved. Its sedimentary record reflects the retrogradation of estuarine environments (tidal flats (U3), Tidal Ravinement Surface (S3), and intra to pro-estuarine sand bars (U4/S4/U5)) during the Holocene transgression (ca. 9000 to 7500 cal yr BP). Open marine environments seal up this estuary with the onset of a flat Wave Ravinement Surface (S5) overlain by thin muddy-sands deposits (U6-F2) interpreted as low-energy open marine conditions (4250 to 1800 cal yr BP). Shoreface sands, made up of coarse sands bodies migrating landwards (U6-F3, F4), cover this sedimentary sequence since 1800 cal yr BP.
A numerical interpolation of the picked seimic horizons was proceed to produce seismic isopach maps of sedimentary units and isobath maps of their boundary surfaces. Furthermore, the isobath map of the basal channel topography has enabled us to calculate some geomorphological features (W/D ratio, mean slope, sinuosity index) that characterized the type of channel pattern. The Etel River geomorphological indexes correspond to a straight channel that involves bed-load transportation processes, potentially associated to braided deposits if the sediment load is sufficient. Compared to the Vilaine River, which braided regime is dated at middle Pleistocene in several zones, we assume a possible mainly climatic control for river incisions in Southern Brittany linked to drastical changes in climate regimes occurring during the "Middle Pleistocene Transition".



## 1. Introduction

The Quaternary period is characterized by significant instabilities that resulted in high amplitude sea level oscillations and contrasting glacial and interglacial conditions (Shackleton, 1987). During this period, mid latitude Western Europe alternated between periglacial and humid temperate conditions, and as a consequence, major rivers recorded strong variations in their erosional dynamics and sedimentary loads (Gibbard and Lewin, 2009; Toucanne et al., 2009). Similarly, infilled incised valleys buried in continental shelf sequences constitute important witnesses to the combined effects of high amplitude sea level oscillations driven by climate change and tectonic uplift variations along valley courses (Schumm, 1993; Miall, 1996). What is more, the position of inner shelf incised valleys on the oscillating shoreline zone results in great variations of environment deposits on a vertical, allowing detailed reconstitutions of paleo-bathymetrical evolution. The eustatically-driven oscillation between terrestrial and marine sedimentary conditions controls the position and timing of depositional and erosion processes within incised valleys on the continental shelf (Ashley and Sheridan, 1994; Zaitlin et al., 1994; Foyle and Oertel, 1997; Dalrymple and Choi, 2007).

On the French Atlantic coast, the study of incised valleys preserved in shelf sequences has been mainly based on widely-spaced high resolution

* Corresponding author at: GMGL, UMR 6538 CNRS Domaines Océaniques, Université de Bretagne Sud, Centre de recherche Yves Coppens, Campus de Thoannic, 56017 Vannes cedex, France.
*E-mail address:* guilhem.estounes@gmail.com (G. Estournès).

0025-3227/$ – see front matter © 2012 Elsevier B.V. All rights reserved.
http://dx.doi.org/10.1016/j.margeo.2012.08.005

seismic records, supplemented with sparse shallow cores (Bouysse and Horn, 1968; Pinot, 1974; Vanney, 1977; Allen and Posamentier, 1993; Lericolais et al., 2001; Proust et al., 2001; Féniès and Lericolais, 2005; Chaumillon and Weber, 2006; Menier et al., 2006, 2010; Chaumillon et al., 2008). Proposed models consist in 2D qualitative models that present the general sedimentary succession and 2D geometrical relations between each seismic/sedimentary unit. However, incised valleys are three-dimensional negative topography along which channel morphologies and deposition/erosion processes evolve. Onland, studies of incised valleys generally encompass the characterization of channel morphologies based on the analysis of geometrical features (Schumm, 1985, 1993; Bonnet, 1998; Bonnet et al., 2000; Blum and Törnqvist, 2000) enabling paleo-hydrodynamic and regional uplift considerations. Consequently, even if bi-dimensional sedimentary model can synthetize general erosion/sedimentation history, a three-dimensional vision of the system allows an accurate and factual characterization of seismic facies distribution and seismic unit shapes that should be defined for a better sedimentary interpretation; it then represents the next step in its understanding; What is more, a three-dimensions reconstitution gives an access to a long-stream geomorphological features of the incised-valley system that is a key aspect for the characterization and understanding of a channelized system and its integration in an offshore/onland geological pattern.

The recent acquisition of a regular (rectangular pixels) and dense grid of 2D high-resolution seismic profiles (150×200 m) covering a total area of 16 km$^2$, coupled with GIS software now affords to propose a revised three-dimensional consideration of the Etel River valley on the inner shelf of the Armorican Massif.

The goal of this article is then to propose i) an updated three-dimensions sedimentary model of a currently drowned paleo-river based on 2D seismic reflexion profiles, ii) leading to new constraints on paleo-geomorphology of this paleo-valley in order iii) to integrate this drowned paleo-valley system to the regional and onland drainage system. This study focuses on the drowned paleo-Etel Channel that has been densely covered by seismic surveys (Menier et al., 2006; this study) making possible an accurate interpolation between seismic profiles in order to reconstitute paleo-morphologies (surfaces and sedimentary volumes).

## 2. Regional setting

### 2.1. Geomorphic setting of the Bay of Etel

The Bay of Etel is located south of the Armorican massif (between latitudes 47°30′ to 47°43′ N and longitudes 3°10′ to 3°25′ W), and is bounded to the west by the mouth of the Blavet and the south-east by the Quiberon Peninsula (Fig. 1). This physiographical unit belongs to the "inner regions" defined by Vanney (1977). The "inner regions" or "*précontinent Breton*" of Pinot (1974) are situated between the coast and the −50 m isobaths of marine maps, and underlies the area of this study. It forms the inshore drowned extension of the currently emergent Armorican Massif, topographically marked by the incision of paleo-river networks by opposition to the offshore "central and outer regions" which present purely marine morphologies characterized by flat topographies (Vanney, 1977).

These "inner region", varying in width from 5 to 14 km, comprise two sectors (Fig. 1A, B): (1) an inshore sector, with water depths shallower than 30 m, made up of bays (Lorient, Quiberon and Vilaine); and, (2) an offshore sector grossly bounded by the isobath curve −50 m, strewn with islands (Belle-Ile, Groix, Houat, Hoëdic, etc.) and shoals (Plateau de Toulven, Plateau des Birvideaux) which act as a barrier to the dominant south-westerly swell, dissected by filled paleo-river valleys (Guilcher, 1948; Pinot, 1974; Vanney, 1977; Menier, 2004; Menier et al., 2006). In the offshore direction, the incised valley networks taper off below −50 m water depth and pass into a regionally flat marine erosional surface, which defines the central regions (Vanney, 1977).

The modern hydrodynamic regime is represented by a tidal range of 4–5 m and mean significant wave height of 2 m generally directed at east-south-east to east-north-east (Tessier, 2006). Despite its high tidal range and its exposition to North Atlantic swells, induced currents are rather weak in the bay of Etel (<10 cm/s) due to its sheltered configuration behind Groix Island (Lazure and Salomon, 1991). Longshore drift acts from north-west to south-east along the coast.

The Etel River downcuts into Tertiary formations composed of sandy calcarenite of Bartonian age and the Hercynian crystalline basement, and the valleys are eroded in a NE–SW orientation. Two major paleo-drainage networks have been interpreted from seismic section in the north-eastern half of the network: one adjacent to the mouth of the modern Etel River, and the other farther to the south-west. These buried channels lead into valleys ranging in width between 200 m and 1500 m, which follow a sinuous to rectilinear thalweg, and which join at around 40 m water depth 15 km from the coast to form a single channel (Fig. 1). At a regional scale, the drainage network is of semi-dendritic type (Menier, 2004; Menier et al., 2006).

The Bay of Etel is bounded in the north by a sand ridge (beaches and dunes) that extends from Gâvres to the isthmus of Penthièvre (Fig. 1). The surface sedimentary cover has been investigated by many earlier studies, e.g. Pinot (1974), Vanney (1977) and Chassé and Glémarec (1976).

### 2.2. Geological setting

Southern Brittany shelf occurs on the passive margin of the northeastern Atlantic, formed by the opening of the Bay of Biscay by rifting at the end of the Early Cretaceous (Aptian/Albian) (Montadert, 1979; Olivet, 1996). The sedimentary cover sequence is carbonated dominated with punctuated terrigenous episodes between Late Cretaceous and Late Miocene (Preux, 1978-Puit PENMA 1; Thinon et al., 2008). High amplitude oscillations of the mean-sea level during the Quaternary, associated with strong climatic variability, are usually considered as the main cause of shallow incision of river valleys at the top of these Neogene formations (Bouysse and Horn, 1968; Pinot, 1974; Delanoë et al., 1975, 1976; Vanney, 1977; Menier et al., 2006). On the French Atlantic shelf, the valley network tapers below −50 m in depth (Pinot, 1974; Vanney, 1977; Lericolais et al., 2001; Proust et al., 2001; Chaumillon et al., 2008; Menier et al., 2010). In most cases, the valley infillings correspond to a Holocene transgressive sequence passing from estuarine to marine deposits (Chaumillon et al., 2008; Sorrel et al., 2010). Locally, fluvial lowstand deposits are also preserved on the valley floor and flanks (Allen and Posamentier, 1993; Lericolais et al., 2001; Proust et al., 2001; Menier et al., 2006).

Below 50 m water depth river incisions disappear in favor of a widespread regional marine ravinement surface overlain by meter-scale thick sand layers and megadunes (Bouysse and Horn, 1968; Pinot, 1974; Vanney, 1977; Lericolais et al., 2001).

On the Southern Brittany inner shelf (0 to −50 m water depth), the ages of the incisions and infillings are still debated because of the radiocarbon dateable material. In the Bay of Etel/Bay of Lorient (Fig. 1A, B) the timing of incision is speculative and could correspond to a diachronous surface shaped during the sustained periods of lowered sea level between the middle and late Pleistocene (Menier et al., 2006, 2010). The sedimentary infill is attributed to the last post-glacial transgression and is composed of tidal muddy sands deposits passing upwards to marine coarse sand sheets (Chaumillon et al., 2008; Sorrel et al., 2010). However, a basal unit interpreted as braided river deposits is punctually identified on the valley floor (Menier, 2004; Menier et al., 2006, 2010).

The better-known river system (both onland and offshore) is the Vilaine River, which is also the most important in term of drainage area (10,000 km$^2$). Its present-day mouth is located 50 km south-eastwards from the Etel River system. The Vilaine River sedimentary filling shows a compound filling constituted with two incomplete

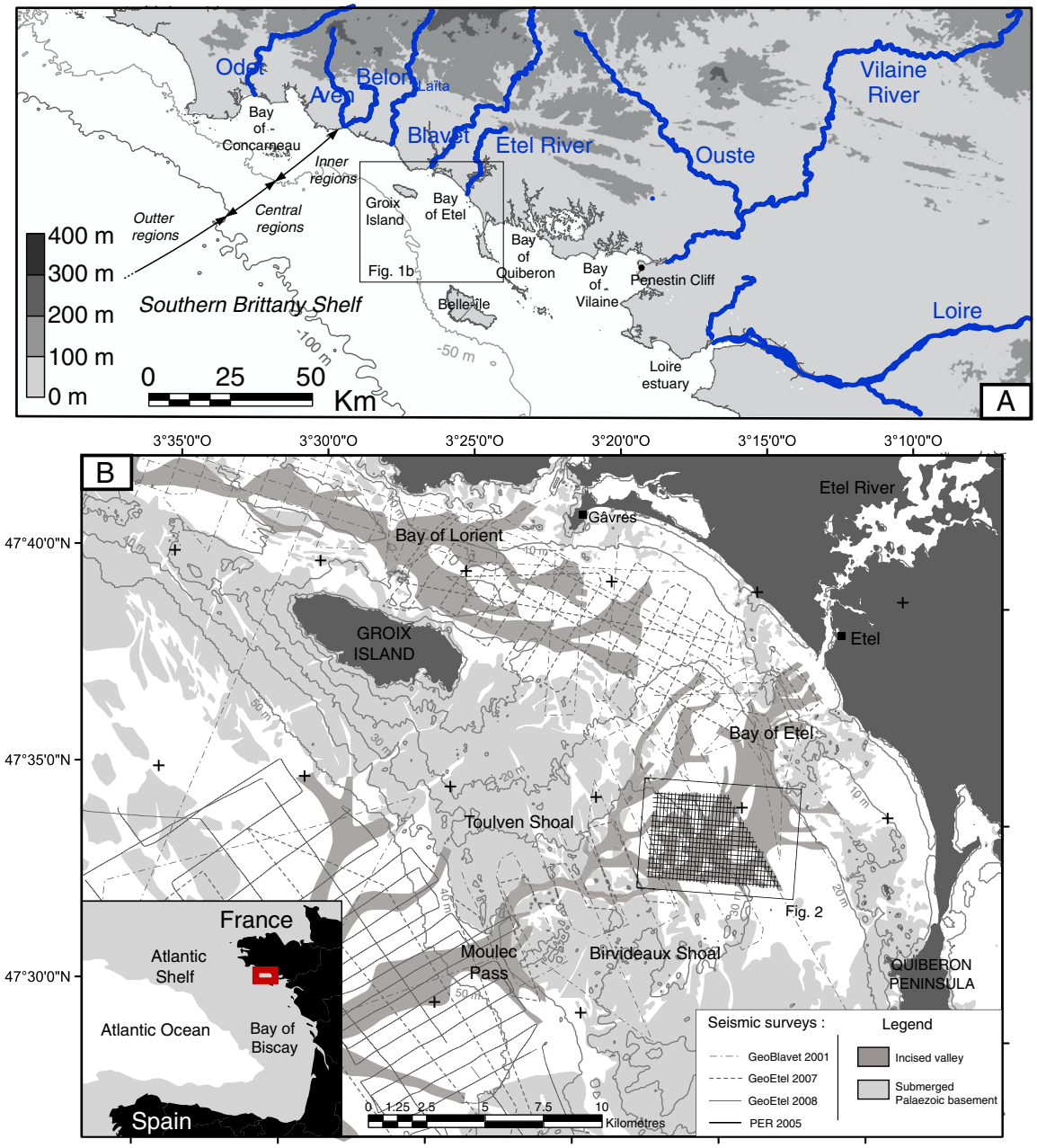


**Fig. 1.** A) Regional location map. "Inner regions", "Central regions" and "Outer regions" according to Vanney (1977). B) Location map of the seismic surveys carried out between 2001 and 2008 on the southern Brittany inner shelf. Location of paleo-valleys networks based on Menier, 2004 and Menier et al., 2006. Distance between bathymetric curves: 10 m (Service Hydrographique et Océanographique de la Marine). Location of rocky outcrops: S.H.O.M. Projected coordinates system: French Lambert 2 extended.

sedimentary sequences. The basal sequence is interpreted as a braided river system dated at 317–600 ky BP by ESR method (Van Vliet-Lanoë et al., 1997; Brault et al., 2004) also recognized in the drowned paleo-Vilaine valley on the inner shelf (Proust et al., 2001). The overlying undated sequence corresponds to a sinuous fluvial system, capped by early Holocene estuarine sediments passing upwards to muddy offshore deposits (Proust et al., 2001; Menier et al., 2006; Sorrel et al., 2010).

## 3. Methodology

### 3.1. Seismic data

This study makes use of 156-line km (59 separate profiles) acquired by high-resolution seismic reflection within the framework of the "South Lorient Exclusive Research Project" (referred to here as ERP), obtained by the Lafarge Company in 2005 (acquisition by the design office Astérie). This campaign supplements the high-resolution seismic data from the missions GeoEtel 2007 and 2008, and GeoBlavet 2001 (Fig. 1) acquired by the "Geosciences Marine et Geomorphologie du Littoral" of the Université de Bretagne Sud, and by the UMR 6118 Géosciences Rennes (University of Rennes 1) aboard the CNRS/INSU vessel "Côtes de la Manche". The data presented in this article were gathered using a monotrace SIG sparker array with a power of 750 J, and were positioned by GPS with meter-scale resolution. These profiles form a regular grid that covers an area of ~16 km$^2$, with rectangular cells having dimensions of 200 m N–S and 150 m E–W (Fig. 2). The interpretation of the seismic reflection data were carried out according to the principles of seismic stratigraphy developed by

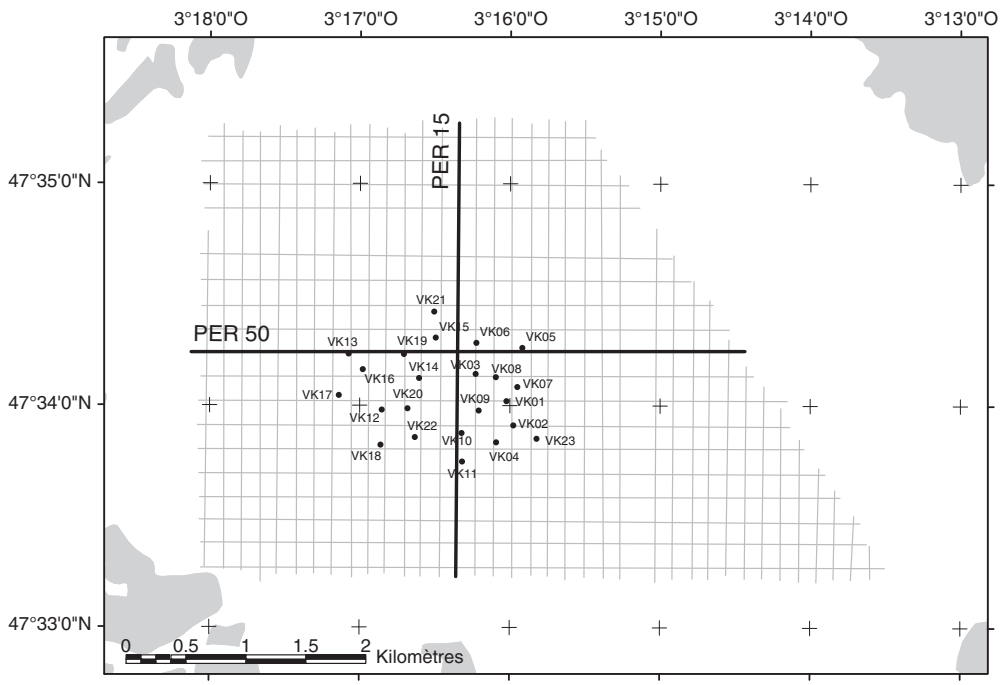


**Fig. 2.** Seismic positioning grid for PER 2005 survey (59 profiles) and the 23 vibro-cores. Bold lines show the location of profiles PER15 and PER50 interpreted in Fig. 4.

Mitchum et al. (1977) and Vail et al. (1977) applied to high-resolution seismic (Table 1).

### 3.2. Digital elevation models creation

The dense regular grid of seismic profiles (Fig. 2) allows the reconstitution of the topography of boundary surfaces to create isobath maps by interpolation of seismic reflectors on 2D seismic profiles. For one reflector, the conversion from 2D seismic data to a 3D interpolated surface required: (a) georeferencing of the 2D surface to be considered (free software Kogeo Seismic Toolkit); (b) interpolation of these picked seismic horizons between seismic profiles. A *triangulated irregular network* (TIN) method was used in this study (Caumon et al., 2009). This isochron TIN surface was converted to raster format discretized at a 23 m resolution; and (c) conversion to *two way travel time* (TWTT) to depth using an estimated velocity of 1500 $m \cdot s^{-1}$ in the water layer and 1800 $m \cdot s^{-1}$ in the soft sediment filling (Nafe and Drake, 1961) (see Fig. 3A for the time to depth conversion calculation). Isobath maps (expressed in meters below the seabed) for particular boundary surfaces were produced. In this article, bathymetric values are always stated according to the present-day isobath 0 m of French marine maps defined as the *lower astronomical tide* level (LATL) on the area.

### 3.3. Geomorphological indices

The creation of isobath maps allowed the characterization of paleo-topographies following the analysis methods of Nordfjord et al. (2005). On each interpolated surfaces, we measured depth below the seabed (minimum and maximum), mean slope and altitude standard deviation (Table 2). Channel morphologies were characterized by channel sinuosity index (P) (Fig. 3B, Table 3) and width on depth ratio (W/D) (Fig. 3C, Table 3) (Rosgen, 1994; Miall, 1996; Nordfjord et al., 2005). W/D calculations are based on width values measured at bankfull stage and channel mean depth (Fig. 3C, Table 3). Due to subsequent reincision and poor preservation of terrace levels, bankfull stage is sometimes barely visible. In that case, width values are taken at the point of slope break in the perpendicular channel section, suggesting a transition between bankfull channel and flood plain environments.

### 3.4. Vibrocores data

#### 3.4.1. Facies sedimentology

Twenty-three vibrocores (maximum 1 m long) were collected within the South Lorient ERP survey area (Fig. 2), and sedimentary facies were described. These lithological data made it possible to establish the

**Table 1**
Description of the main seismic features of each seismic facies encountered in PER 2005 profiles. This description follows the methodology and terms described in Mitchum et al., 1977.

| | Seismic facies | Continuity | Amplitude | Frequency | Configuration | Lower reflection terminations | Upper reflection terminations | Thickness (ms) |
|---|---|---|---|---|---|---|---|---|
| U6 | Fs6b | High to medium | High to medium | Low | Tangential oblique | Downlap | Toplap | 5 |
| | Fs6a | Low | Low | High | Chaotic | / | Truncation | 5 |
| U5 | Fs5b | Medium | High to medium | Low | Subparallel | Conformable | Truncation | <5 |
| | Fs5a | Medium to low | Medium to low | Low | Parallel Oblique | Downlap | Toplap and truncation | 5 to 10 |
| U4 | Fs4c | Low | Medium | Medium | Chaotic/oblique | Downlap | Truncation | 5 |
| | Fs4b | Medium to low | Low | Medium | Parallel oblique | Downlap/onlap | Truncation and toplap | 5 |
| | Fs4a | Low | Medium | medium to low | Subparallel | Conformable/onlap | Truncation | 5 |
| U3 | Fs3b | High to medium | High to medium | Low | Aggrading oblique | Downlap to conformable | Truncation | 5 |
| | Fs3a | High | High | Low | Parallel aggrading | Conformable/onlap | Truncation | 5 to 10 |
| U2 | Fs2b | Medium | Medium | Low | Parallel and folded | Conformable/onlap | Truncation and toplap | 5 |
| | Fs2a | High | High | Low | Parallel and folded | Conformable/onlap | Truncation and toplap | 10 to 15 |
| Ul | Fsl | Medium | High | High to medium | Chaotic | / | Truncation | |

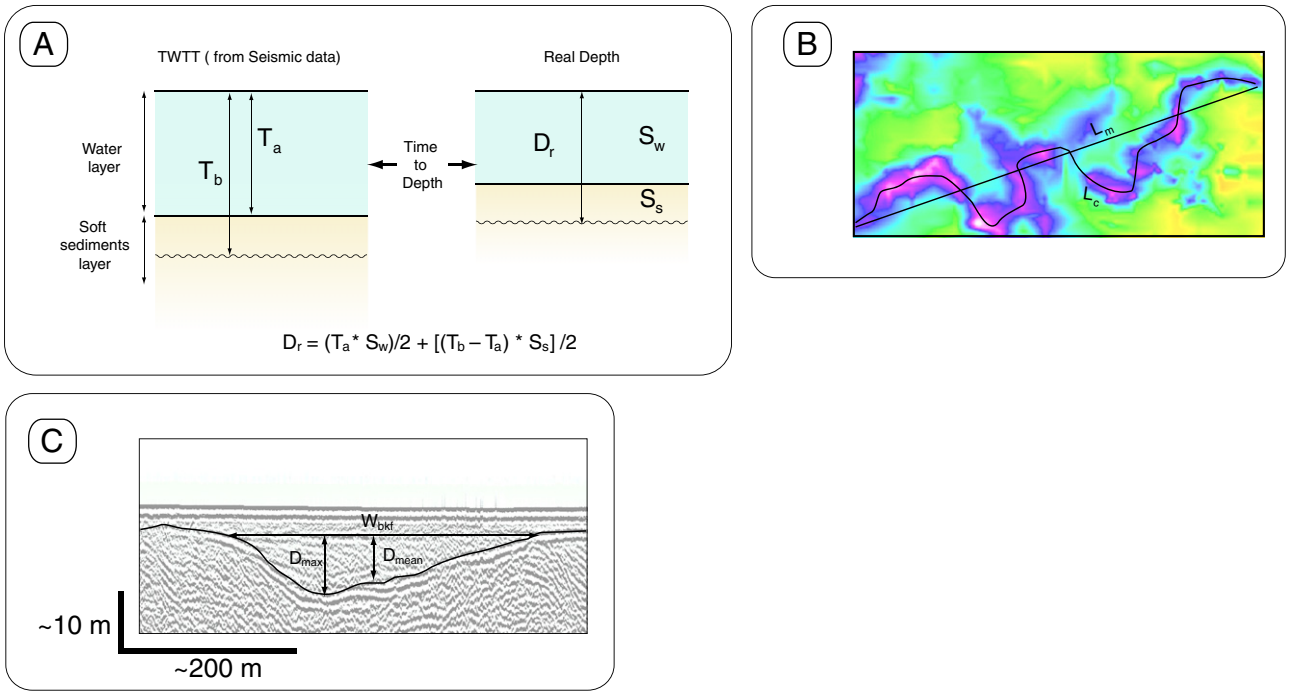


**Fig. 3.** Geomorphological features extracted from DEM based on seismic surfaces. A) Calculation method for the time to depth conversion of seismic surfaces applied to each cell on each surfaces. Dr = depth value corrected from sound speed variations in a multilayer system (m below the lowest tide level Lwtl), Ta = two way travel time between sea floor and Lwtl (ms TWTT), Tb = two way travel time between a surface in sediments and Lwtl (ms TWTT), Sw = speed of sound in salted water (m/s), Ss = speed of sound in soft sediments (m/s). B) Sinuosity index measure. P = sinuosity index, Lm = meander length measured between channel terminations, Lc = channel length measured along the thalweg. C) Width/depth ratio. $W_{bkf}$ = channel width at bankfull depth, $D_{mean}$ = mean depth in the bankfull channel.

succession of depositional environments in the two most recent seismic units (Fig. 4).

*3.4.2. Foraminiferal content analysis*

Foraminifera were extracted from 8 samples taken from VK16 core, which recovered the most undisturbed and complete stratigraphy. Each sample was washed over 45 μm, 125 μm, 500 μm and 2 mm sieves and dried in an oven at 45 °C. Splitting and picking were conducted to obtain about 300 benthic foraminifera from the 125 μm residue. Only six samples contained between 100 and 300 foraminifera, and therefore, were statistically reliable for a paleo-environmental determination purposes (after Fatela and Taborda, 2002). Broken, poorly preserved, pyritized and transported (abraided) specimens were categorized for each species (Table 4). Identifications were based on various taxonomic references (Redois, 1996; Murray, 2003; Perez-Belmonte, 2008) and interpretations of assemblages (Table 5) were carried out using ecological data (Fatela, 1995; Goubert, 1997; Perez-Belmonte, 2008) or morphofunction method for the sparsely documented species (Severin, 1983; Bernhard, 1986; Duleba et al., 1999; Goubert et al., 2001).

*3.4.3. $^{14}C$ dating*

Age determinations were carried out on broken shells taken on cores, yielding twelve ages. Dates were obtained by liquid scintillation counting at the Environmental Isotope Laboratory of the University of Tucson, Arizona (Polach et al., 1973) and two ages (Erl-12798 and Erl-12799 — Table 6) dated at the C-14 AMS laboratory of Erlangen (Germany). The conventional ages are calibrated using the Marine04 curve (Calib software v5.0.1; Hughen et al., 2004), and corrected for local reservoir effects according to the values obtained for the Arcachon Basin (Broecker and Olson, 1961 in Stuiver et al., 2005): delta-R of +265 years with a standard deviation of ±44 years. Mean calibrated ages (expressed in calendar years before present) are derived from the two sigma range (Table 6).

**Table 2**
Geomorphological parameters of the boundary surfaces.

| Surface | Maximum depth (m) | Minimum depth (m) | Altitude standard deviation | Mean slope (%) |
|---|---|---|---|---|
| S6 | −36 | −25.5 | 2.2 | 0.87 |
| S5 | −38 | −28 | 1.4 | 0.7 |
| S4 | −44 | −29 | 2.1 | 1.05 |
| S3 | −48 | −28.5 | 3.2 | 1.92 |
| S2 | −48 | −29 | 4.2 | 2.27 |
| S1 | −72 | −31 | 6.2 | 3.67 |

## 4. Results

### 4.1. Holocene seismic stratigraphy

The seismic-stratigraphic analysis reveals the existence of five boundary reflectors that delineate six seismic units. Seismic units can be further subdivided into eleven seismic facies (Table 1).

*4.1.1. Seismic boundary surfaces*

Surface S1: This reflector forms a lowermost erosive boundary between the metamorphic basement and the overlying sedimentary cover. It strongly dips towards the south-west and presents high altitudinal variations (Fig. 5A, Table 2). This surface cannot be continuously picked out because of subsequent truncations. This latter is offset by a N160 trending fault with a vertical throw of 30 m. This fault escarpment lowers the south-western basement block compared to the north-eastern part (PER 50 — Fig. 4), and forms a half-graben structure preserving Lutetian to Bartonian formations (Thinon et al., 2008).

Surface S2: This surface incises the top of seismic unit U2 (Fig. 4) and locally of U1. It dips towards the south-west and presents high values of altitude standard deviation indicating a strongly dissected topography (Table 2). On

**Table 3**
Geomorphological parameters of channels (see locations of the channels sectors in Fig. 5a).

| Surface | Section | Mean V (m) | Mean D (m) | Mean W/D | Straight length (m) | Channel length (m) | Sinuosity index | Channel shape |
|---|---|---|---|---|---|---|---|---|
| S3 | S3d | 515 | −4 | 145 | 2573 | 2937 | 1.1 | Symmetric V shape |
| | S3c | 370 | −4 | 91 | 3016 | 4642 | 1.5 | Asymmetric V shape |
| | S3b | 497 | −3 | 189 | 2141 | 2884 | 1.3 | Large with multiple internal scours |
| | S3a | 286 | −2 | 131 | 1789 | 2226 | 1.2 | Asymmetric shape |
| S2 | S2d | 621 | −4 | 147 | 2756 | 3220 | 1.2 | Flat bottom |
| | S2c | 370 | −4 | 91 | 3016 | 4642 | 1.5 | Asymmetric V shape |
| | S2b | 668 | −5 | 125 | 1805 | 1954 | 1.1 | Flat bottom |
| | S2a | 386 | −4 | 99 | 1811 | 2082 | 1.1 | Symmetric shape |

seismic sections, the surface is expressed as a pair of continuous reflectors of high amplitude and low frequency (Fig. 4). Mapping reveals a NNE to SSW oriented incision made up of three tributary channels, converging and joining at the south-western part of the study (Fig. 5A). The evolution of the channel section leads to distinguish four different sectors (a, b, c and d zones — Fig. 5A) characterized by different geomorphological indexes (Table 3). The convergence of sectors S2a and S2b leads to S2d sector downdip. The S2c sector joins with S2d to the south, forming a dendritic channel network (Fig. 5A). These channels are generally straight except in S2c that presents an obvious sinuous aspect (Fig. 5A, Table 3). All channel sections show high W/D values (around 100). Two types of sections are represented: (i) S2a and S2c sectors present narrow (380 in width) V shape sections,

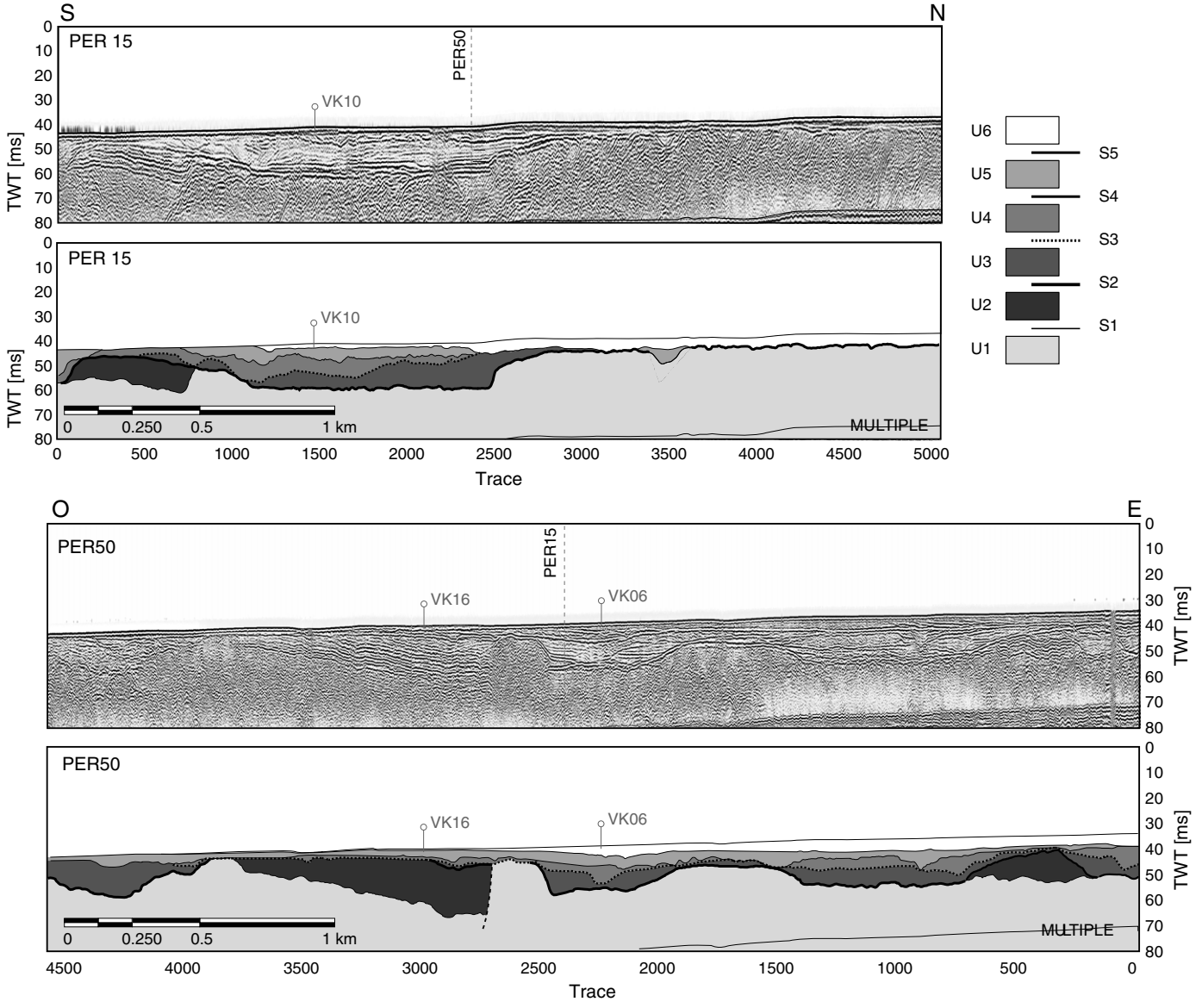


**Fig. 4.** Raw seismic profiles with interpretations in terms of seismic units, stratigraphic surfaces and line drawing (cross sections PER15 and PER50, see location in Fig. 2).

**Table 4**
Faunistic assemblage table showing proportion of each benthic species identified in the core sample.

| | Species |
|---|---|
| Dominant (>20%) | *Asterigerinata mamilla* (Williamson, 1858) |
| | *Cibicides refulgens* (de Montfort, 1808) |
| | *Elphidium excavatum forma lidoensis* (Cushman, 1936) |
| Common (10–20%) | *Quinqueloculina seminula* (Linné, 1758) |
| | *Lobatula lobatula* (Walker & Jacob, 1798) |
| | *Ammonia beccarii* (Linné, 1758) |
| | *Textularia truncata* (Höglund, 1947) |
| Accessory (5–10%) | *Elphidium gerthi* (van Voorthuysen, 1957) |
| | *Haynesina germanica* (Ehrenberg, 1840) |
| | *Elphidium excavatum forma excavata* (Terquem, 1876) |
| | *Rosalina globularis* (d'Orbigny, 1826) |
| | *Gavelinopsis praegeri* (Heron-Allen & Earland, 1913) |
| | *Elphidium advenum* (Cushman, 1922) |
| | *Bulimina marginata* (d'Orbigny, 1826) |
| | *Planorbulina mediterranensis* (d'Orbigny, 1826) |
| | *Quinqueloculina lata* (Terquem, 1877) |
| Rare (1–5%) | *Bulimina elegans* (d'Orbigny, 1826) |
| | *Rosalina vilardeboana* (d'Orbigny, 1839) |
| | *Miliolinella subrotunda* (Walker & Boys, 1784) |
| | *Elphidium excavatum forma selseyensis* (Heron-Allen & Earland, 1911) |
| | *Angulogerina angulosa* (Williamson,1858) |
| | *Brizalina spathulata* (Williamson, 1858) |
| | *Bulimina elongata* (d'Orbigny, 1846) |
| | *Fissurina lucida* (Williamson, 1858) |
| | *Lagena williamsoni* (Alcock, 1865) |
| | *Hyalinea balthica* (Schröter, 1783) |
| | *Nonion fabum* (Fichtel and Moll 1798) |
| | *Triloculinella circularis* (Bornemann, 1855) |
| | *Amphicoryna scalaris* (Batsch, 1791) |
| | *Cycloforina longirostra* (d'Orbigny 1846) |
| | *Quinqueloculina trigonula* (Terquem, 1876) |
| | *Ammonia tepida* (Cushman, 1926) |
| | *Haynesina depressula* (Walker & Jacob, 1798) |
| | *Aubignyna* sp. |
| | *Elphidium crispum* (Linné, 1758) |
| | *Eggerelloides scabrus* (Williamson, 1858) |
| | *Lenticulina* sp. |
| | *Lagena laevicostata* (Cushman & Gray, 1946) |
| | *Favulina melo* (d'Orbigny, 1839) |
| | *Elphidium poeyanum* (d'Orbigny, 1839) |
| | *Elphidium incertum* (Williamson 1858) |
| | *Globigerina bulloides* (d'Orbingy 1826) |
| | *Hoeglundina elegans* (d'Orbigny, 1826) |
| | *Patellina corrugata* (Williamson, 1858) |
| | *Bolivina variabilis* (Williamson, 1858) |
| | *Neoconorbina terquemi* (Rzehak, 1838) |
| | *Elphidium pulvereum* (Todd, 1958) |
| | *Gavelinopsis nitida* (Williamson, 1858) |
| | *Cassidulina laevigata* (d'Orbigny, 1826) |
| | *Cassidulina obtusa* (Williamson, 1858) |
| Accidental (<1%) | *Adelosina* sp. |
| | *Brizalina alata* (Seguenza, 1862) |
| | *Elphidium aculeatum* (d'Orbigny, 1846) |
| | *Globulina gibba* (d'Orbigny, 1826) |
| | *Massilina secans* (d'Orbigny, 1826) |
| | *Trifarina bradyi* (Cushman, 1932) |
| Reworked species | Miliolids |
| | Cibicids |
| | *Nonionella turgida* (Williamson, 1858) |
| | *Spiroloculina circularis* (Cushman, 1921) |
| | *Elphidium clavatum* (Cushman, 1930) |
| | *Elphidium williamsoni* (Haynes, 1973) |
| | *Spirillina vivipara* (Ehrenberg, 1843) |
| | *Gyroidina orbicularis* (d'Orbigny, 1826) |
| | *Melonis barleanus* (Williamson, 1858) |

respectively symmetric and asymmetric while (ii) S2b and S2d sectors are characterized by flat bottom channel associated to steep flanks and large sections exceeding 600 m in width (Table 3).

Surface S3: This surface dips to the south-west along a mean slope of 1.9% (Table 2). Its seismic signature consists of one reflector presenting poor to average continuity of medium amplitude (Fig. 4). S3 is totally confined within S2 channel boundaries and then shows an almost similar contour line (Fig. 5A). Its relatively high altitude standard deviation value (Table 2) indicates a topographically rough surface marked by concave-up "pool" morphologies in sectors S3a, b and c (Fig. 5A). Pools are 3 to 4 m deep, occupying the whole channel width and stretching over several hundreds of meters along the channel direction (Fig. 5A). Pools length and depth tend to increase downdip, thinning to a minimum of 2 m above the basement incision surface S2. In comparison to S2, W/D values increase due to a moderate narrowing of ca. 100 m of the channel width associated to lower values of bankfull depth (Table 3). Out of the channels, S3 merges with S2 and S1 forming a regular sub planar surface on the basement.

Surface S4: This surface occurs as paired reflectors of medium amplitude and continuity (Fig. 4). It is also distinguished by being smooth with a two times lower mean slope compared to S2 and S3 (Table 2). Narrow and shallow channel incisions are superimposed over part of the former stream directions (sectors b and d). However, unlike S3, this channel does not occupy the whole width of the former channel S2. On the other former channel sectors (sectors a and c), S4 appears as a flat erosional surface locally truncated by the overlying surface S5 (Figs. 4 and 5A).

Surface S5: It is the first surface that does not show any localized incision. This surface has the lowest altitude standard deviation value (Table 2) and shows a gentle slope to the south-west. It truncates all the underlying deposits as a flat horizontal erosional surface and sub-crops in the south-western part of the studied zone. On seismic profiles, it is represented by a couple of highly continuous reflectors with high amplitude and low frequency (Fig. 4).

Surface S6: This reflector is the current sea floor with a mean depth of −30 m across the study area, gently dipping to the south-west (Table 2) as a smooth surface.

#### 4.1.2. Seismic units

Seismic unit U1: This unit composes the basement that underlies all the other sedimentary units visible in the top 40 ms of the seismic section (Fig. 4). It is bounded upwards by the S1 surface and extends beneath the seafloor multiple. It seismic facies appears chaotic at very high frequency, sometimes with steeply dipping reflectors, locally folded, as well as many diffraction parabolas (Fs1) (Table 1). This unit has regional extent and is classically interpreted as the Hercynian meta-sedimentary basement made up of mica schists, amphibolites and blue schist facies of the Groix–Céné Unit (Thinon et al., 2008). This unit crops out on the seabed only in the north of the study area.

Seismic unit U2: This unit overlies the regional erosion surface S1, with the contact showing none through to a strong angular unconformity. The top of the unit is truncated by the erosive surfaces S2 and S3 (Fig. 4). Unit 2 is particularly well represented within half-grabens where reflections folding and tilting towards the east (Fig. 4). Its reflectors are locally offset by the fault escarpment that bounds the half-graben the east, described above (U2, Fig. 5B). Two seismic facies can be distinguished: (i) the seismic facies Fs2a groups highly continuous reflectors of high amplitude and low frequency. (ii) Fs2b facies is equivalent but shows average amplitude and frequency (Table 1). The mean thickness value of U1 reaches 7 m but exceeds 30 m within the

**Table 5**
Definition of the 17 ecological groups. Position of each group in core VK16 is given in Fig. 3.

| Ecological group | Species |
|---|---|
| EG 1 *Haynesina germanica* | |
| EG 2 *Globigerina bulloides* | |
| EG 3 *Bolivina* + *Brizalina* | *Bolivina variabilis*, *Brizalina alata*, *Brizalina spathulata* |
| EG 4 *Elphidium gerthi* | |
| EG 5 Others *Elphidiuin* | *E. aculeatum*, *E. advenum*, *E. crispum*, *E. incertum*, *E. pulvereum* |
| EG 6 *Hyalinea balthica* | |
| EG 7 Infaunal | *Angulogerina angulosa*, *Globulina gibba*, *Trifarina brady* |
| EG 8 Epifaunal (and shallow infaunal) | *Aubignyna*, *Cassidulina*, *Favulma*, *Fissurina lucida*, *Havnesina depressula*, *Hoeglundina elegans*, *Lagena*, *Leuticulina*, *Nonion fabuni* |
| EG 9 *Bulimina* spp. | *Bulimina marginata*, *B. elongata* |
| EG 10 *Quingueliculina senunula* | |
| EG 11 Others porcelaneous | *Adelosina*, *Clycloforina longirostra*, *Massilina secans*, *Miliolinella subrotunda*, *Quingueliculina lata*, *Q. trigonula*, *Triloculmella circulans* |
| EG 12 *Asterigerinata*, *Gavelinopsis*, *Lobatula* | *Asterigerinata mamilla*, *Gavelinopsis praegeri*, *Lobatula lobatula* |
| EG 13 *Cibicides refiilgens* | |
| EG 14 Others epiphytic | *Neoconorbina terquemi*, *Patellina corrugata*, *Planorbulina mediterranensis*, *Rosalina globularis*, *R. vilardeboana* |
| EG 15 *Textularia truncata* | |
| EG 16 *Ammonia beccarii* | |
| EG 17 *Elphidium excavatum* gr. | *E. excavatum forma clavatum*, *forma selseyensis*, *forma excavata*, *forma lidoensis* |

half-graben and trough structures (Fig. 5B). This unit is of regional extent and has been interpreted previously as detrital limestone and dolomitized sands (Gros and Limasset, 1984; Borne and Chevalier, 1986). It has been initially attributed to the Upper Lutetian (Andreiff et al., 1968; Bouysse and Horn, 1968; Delanoë et al., 1975). Biostratigraphically Unit U2 would belong to the Lower to Middle Bartonian (Hardenbol et al., 1998 in Guillocheau et al., 2003).

Seismic unit U3: This unit overlies U1 and U2 through the erosive surface S2. This unit is entirely confined within S2 channels and is of 1 to 6 m in thickness general, but locally exceeds 12 m in the deepest incisions (Fig. 5B). It lies para-conformably or downlaps at the center of the S2 channels and onlaps the channels flanks (Fig. 4). Unlike U2, reflectors within U3 are neither folded nor tilted suggesting deposition subsequent to the deformation phase that affected U2 (Fig. 4). Stratification is marked by continuous high amplitude and low frequency reflections. U3 is composed of two seismic facies: Fs3a presents horizontal aggrading reflectors passing in the southern part of S2 channel (S2d sector) to sub parallel aggrading and prograding oblique stratifications downlapping on S2 surface.

Fs3a is mainly preserved within the sectors S2a, b and locally c. In the sector S2d, the deposition of U3 proceeds from the convergence of two sedimentary bodies migrating from S2 valley flanks to the center of the channel delineating an internal channel within U3 (Fig. 6A, B). The full extent of the channel incision is not ubiquitously preserved and is often truncated by the overlying erosional surface S3. This symmetrical channel is 100 m wide and reaches 5 m deep; it appears to be maintained while lateral edges continue to grow by aggradation/progradation processes. Downdip, in the southern part of S2d, progradation takes over aggradation in deposits pattern and leads to the progressive decline of the eastern bench. As a consequence, the internal channel tends to move eastwards and to enlarge, passing to 200/250 m in width (Fig. 6A, B).

Seismic unit U4: This unit infills the S3 channel incision and is bounded upwards by the erosive S4 surface and locally by S5. U4 has an average thickness of 6 m at the center of the channels but can locally reach >10 m (Fig. 5B). It is made up of three seismic facies showing discontinuous reflectors with low to medium amplitude and frequency (Table 1). Reflector terminations vary depending on the geometry of the channels they fill: in the narrower channel sections (S3a), reflectors are para-conformable and onlap the channel flanks (Fs4a). Elsewhere (S3b, c and d), the filling shows prograding oblique reflections (Fs4b), sometimes associated to chaotic configurations (Fs4c) particularly

**Table 6**
Radiocarbon dates for the vibrocores sampled in the Bay of Etel (see Fig. 2 for core locations and Fig. 6 for location of dated samples from cores). N/A: not available.

| Labcode | Sample code | Core depth (m) | Sample position in core (m) | Conventional date (radiocarbon years BP) | $\delta^{13}C$‰ | Calibrated age 2 sigma (cal years BP) | Mean calibrated age (cal years BP) |
|---|---|---|---|---|---|---|---|
| 14901 | VK2A | −30.3 | −30.5 | 6275 ± 100 | 0.6 | 6208–6675 | 6442 ± 234 |
| 14902 | VK6A | −29.9 | −30.2 | 2460 ± 60 | 0.8 | 1600–1974 | 1788 ± 188 |
| 14903 | VK6B | −29.9 | −30.4 | 18,105 + 335/−325 | 1.3 | 19,862–21,543 | 20,703 ± 841 |
| 14904 | VK1OA | −30.9 | −31.3 | 15,495 + 475/−445 | 1.1 | 16,564–18,938 | 17,752 ± 1188 |
| 14905 | VK16A | −30.9 | −31.2 | 7255 ± 115 | 0.9 | 7254–7702 | 7479 ± 225 |
| 14906 | VK16B | −30.9 | −31.3 | 4450 ± 105/−100 | 0.8 | 3931–4571 | 4252 ± 321 |
| 14907 | VK16C | −30.9 | −31.5 | 4470 ± 85 | 0.3 | 4003–4548 | 4276 ± 273 |
| 14908 | VK2OA | −30.8 | −31.3 | 6635 ± 110 | 08 | 6570–7149 | 6860 ± 290 |
| 14909 | VK2OB | −30.8 | −31.5 | 7635 ± 155 | 1 | 7542–8165 | 7854 ± 312 |
| 14910 | VK22A | −31 | −31.2 | 8525 ± 100 | 0.8 | 8503–9092 | 8798 ± 295 |
| 14911 | VK22B | −31 | −31.8 | 14,010 + 170/−165 | 1 | 15,258–16,416 | 15,838 ± 580 |
| NA | VK14 | −30.6 | −30.9 | 2217 ± 150 | N/A | 1207–1880 | 1544 ± 337 |
| Erl-12798 | Er-1 VK2O | −30.8 | −31.6 | 3062 ± 209 | N/A | 1986–3049 | 2518 ± 532 |
| Erl-12799 | Er-2 VK22 | −31 | −31.7 | 2931 ± 101 | N/A | 2106–2688 | 2398 ± 292 |

where channels are the widest (S3b and S3d). The progradation is generally oriented towards the south-east and more particularly in the S3d section where the channel is the widest.

Seismic unit U5: This unit overlies the S4 surface, covering a weakly incised channel (S4 — see Section 4.1.1) and is truncated at the top by S5 (Fig. 4). U5 is made up of two seismic facies (Table 1): Fs5a downlaps onto S4 by the progradation towards the east of parallel oblique reflections poorly illustrated on seismic section and is 1 to 6 m thick (Fig. 5B). Outside of the S4 channel, U5 forms a thin drape of <3 m thick lying in para-conformably above S4 (Fs5b). This unit subcrops at a few tens of cm under the current seabed in the western part of the study area. Its top has been pierced by the vibro-cores carried out on this zone (Fig. 4). The poor continuity of reflectors results from a coarse grain size that is confirmed by cores.

Seismic unit U6: This seismic unit corresponds to the uppermost part of the sedimentary sequence in the study area, occurring as a wedge that thickness passes from 1 m in the south-west to 7 m in the north-east (Fig. 5B). This sedimentary wedge overlies the sharp horizontal erosive surface S5 (Fig. 4). This unit forms megadunes that migrate in a landwards direction (towards the north-east; Fs6a and Fs6b). The progressive shifting from facies Fs6a to Fs6b does not highlight any change of material nature but reflects changes in the orientation of reflectors.

### 4.2. Cored surface formation description

Vibro cores were taken to sample the top of unit U5 and U6, and the surface S5 (Figs. 4 and 7). The sedimentological descriptions are

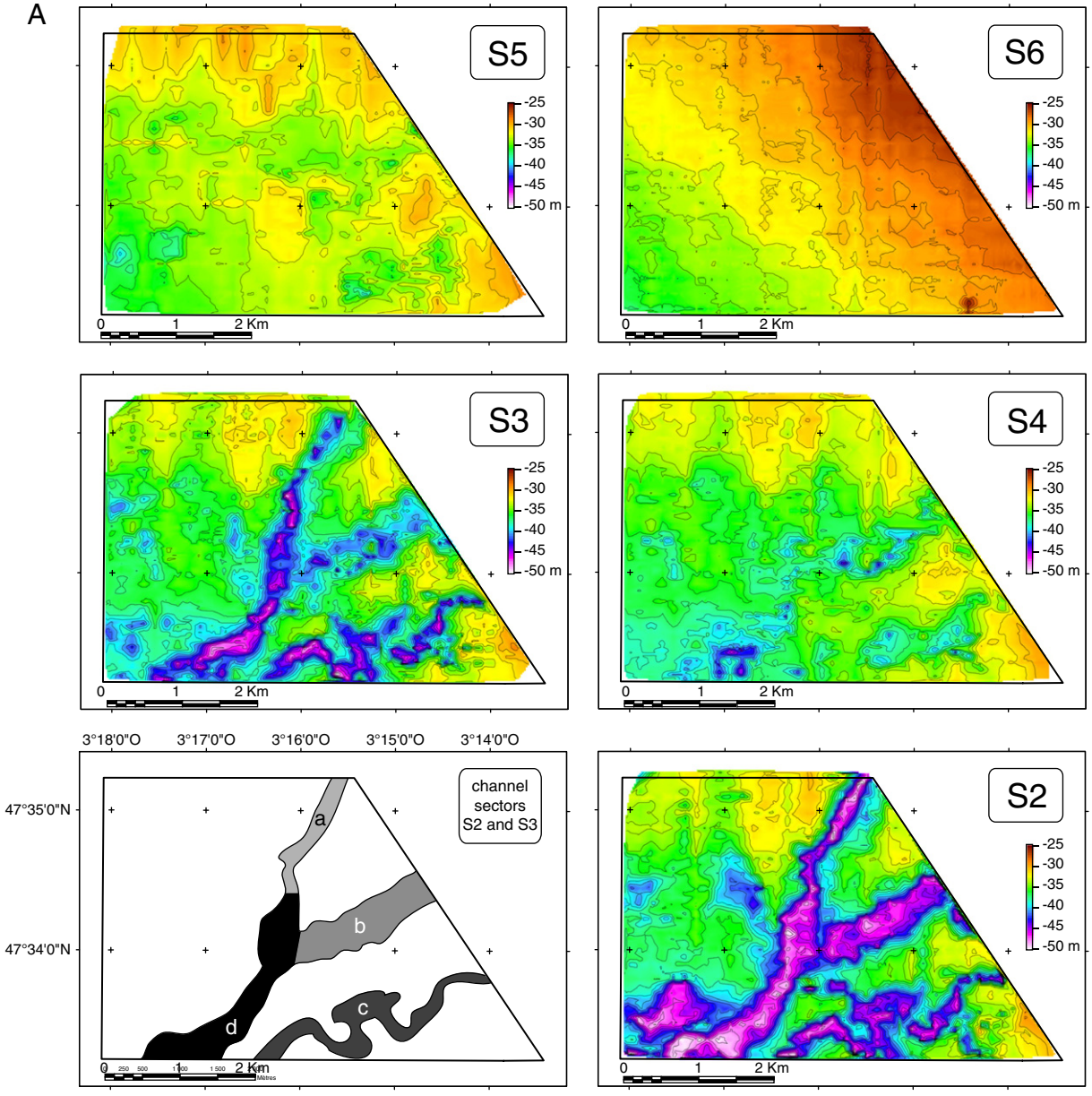


**Fig. 5.** A) Isobath maps for stratigraphic surfaces picked on the 59 seismic profiles. B) Isopach maps for seismic units constructed by subtracting the top and floor surface depth of each unit. Time to depth conversion is based on the assumption of a P-wave velocity of 1600 m/s (value for unconsolidated sediments). This probably underestimates the thickness of U2 (Eocene carbonated sandstones). On U1 map, dotted line represents Thinon et al., 2008 mapping for Middle to Late Eocene formations.

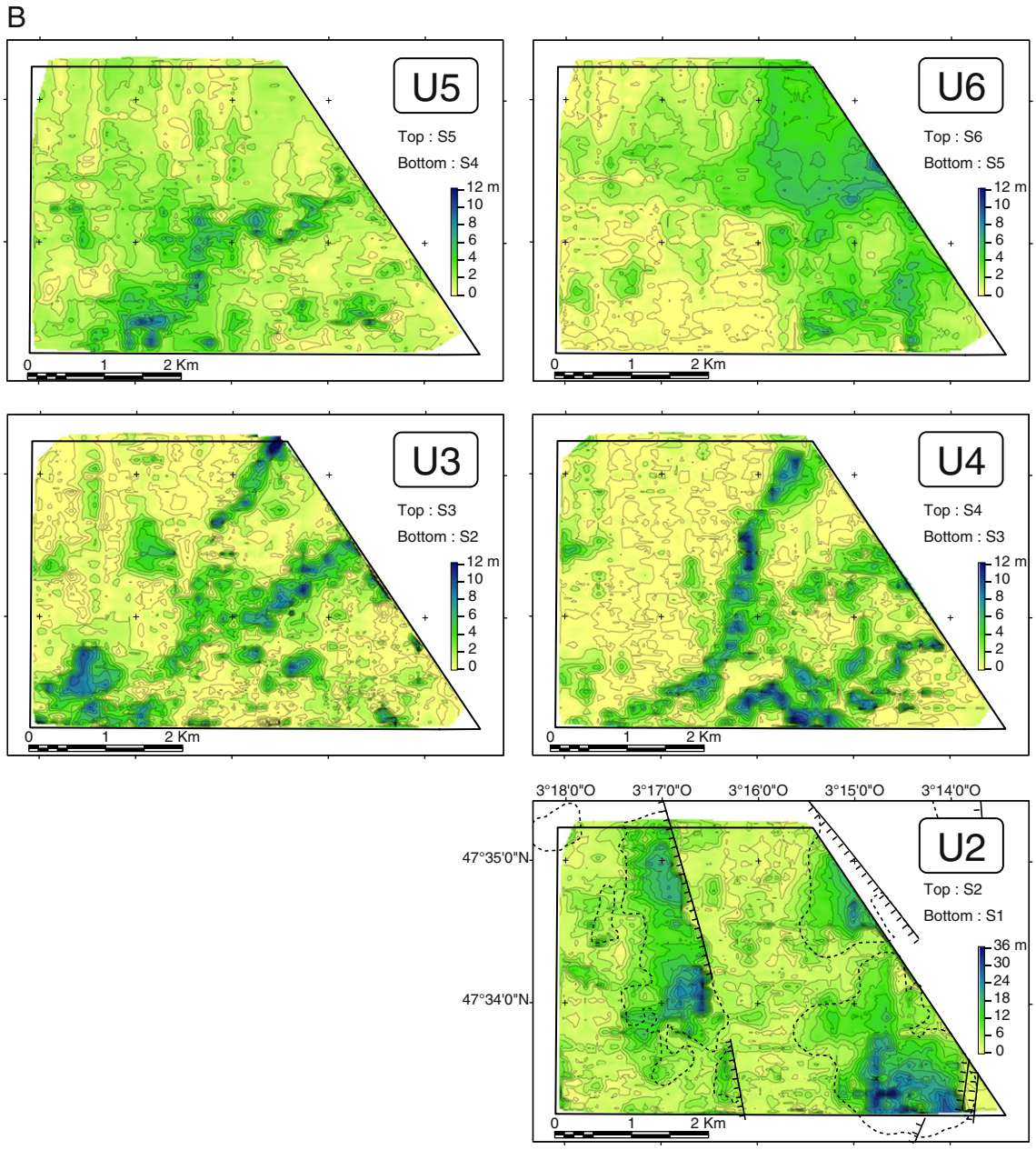


**Fig. 5** (*continued*).

supplemented with foraminiferal content and ecology for eight selected zones in the core VK16 (Fig. 8, Tables 4 and 5). Chronostratigraphical constraints are provided by the fourteen radiocarbon dates that range in age from 1544 to 20,703 cal yr BP (Table 6, Fig. 7). Dated bioclasts propose ages comprised between 20,700 and 15,800 cal yr BP (Table 6, Fig. 7).

*4.2.1. Description of sedimentary facies*

Sedimentary facies F1: This facies corresponds to the top of the seismic unit U5 and occurs at the basal 5 cm of several cores (Fig. 7). It consists of gravels grading locally to quartzite pebbles to form a grain supported, non-cemented micro-conglomerate with rounded to sub-rounded clasts in a silty to muddy matrix. Grains are very poorly sorted, presenting a mean size of 1 cm. Some slightly fragmented to fragmented whitish (decalcified) bioclasts (5 mm maximum) are also present in the matrix, but in small amounts.

The occurrence of well-preserved tests of *Haynesina germanica* (EG1; Tables 4 and 5) in this facies (Spl-1 — Fig. 8) indicates an input of fresh waters and nutrients coming from continental run-off. This continental influence is observed only in facies F1 and would indicate shallow, near-shore environments. The well-preserved and reworked assemblages are characterized by the dominance of epiphytic and epifaunal ecological groups and by hardy species (Fig. 8).

Sedimentary facies F2: This facies often overlies F1, above the erosive surface S5 described on seismic profiles (Fig. 7). It is 10–40 cm in thickness and constitutes the base of the seismic unit U6. This grayish to greenish colored facies is made of three sub facies not represented in every core except in VK16. From base to top:

(a) sub facies F2a is dominated by silty, micaceous, poorly sorted fine to medium sands. The abundant bioclastic content (≈20% of the elements) is of very small size (<1 mm). It is rich in muscovite fragments (<0.5 mm).

(b) sub facies F2b consists in bioclastic accumulations 1 to 2 cm thick intercalated as lenses between F2a and F2c. It forms clast-supported accumulations of strongly fragmented bioclasts (1 to 2 mm). Such layers are not systematically present in every core, just as the number of layers is also variable from core to core. Dating gives various ages (Table 6), implying an intense reworking of shells.

(c) sub facies F2c is a well sorted, dark silty-fine sand. The bioclastic fraction is completely equivalent to that of F2a.

Foraminiferal content analysis was carried out on four samples: Spl-2, Spl-3, Spl-4 and Spl-5 (location in Fig. 8). It is characterized by a relatively high specific diversity according to the occurrence of fifteen ecological groups out of seventeen. Only *H. germanica* (EG1 — Tables 4 and 5) and *Elphidium excavatum* gr. (EG17 — Tables 4 and 5) are not encountered in this facies. The assemblages indicate an open marine environment with slow currents and well-oxygenated waters, compared with the facies F1. Seagrass and all ecological niches are occupied by benthic foraminifers. The occurrence of *Hyalinea balthica* (EG6) could indicate an influx of cold waters. The paleo-water depth is estimated to around 10–20 m. Radiocarbon dates indicate age of 2400–4250 cal yr BP in the F2 facies (Table 6, Fig. 7).

Sedimentary facies F3: This sedimentary facies is a poorly sorted medium to coarse sand that constitutes much of the current seafloor within the study area. It forms meter-scale thick sandy megadunes that overlie the erosive contact at the top of facies F2, and can be easily distinguished by its rust color (Fig. 7). Its thickness ranges from 10 to 50 cm in cores. Bioclastic content reaches 20% of the clast content. Whole shells of bivalves, disarticulated and sometimes colored, are locally preserved but most of the bioclastic content (Fig. 7).

The base is characterized by a low foraminiferal content and by the higher rate of reworked tests (Spl-6). The assemblage is largely dominated by epiphytic and epifaunal species. The two samples from the top of the core (Spl-7 and Spl-8) are characterized by a relatively high specific diversity, but with a low ecological variety. Epiphytic and epifaunal species are dominant and the first occurrence of *E. excavatum* gr. (EG17) is observed in this facies (Fig. 7).

Most of the radiocarbon dates of this facies present older ages than in F2 (Table 6, Fig. 7) suggesting intense reworking of bioclasts. The most recent age is 1800 cal yr BP.

Sedimentary facies F4: This facies is made of sparse muddy to very fine sand accumulations over the studied area which caps a few cores. It represents 40 cm in the core VK14 (Fig. 7). The only available date indicates an age of 1550 cal yr BP (Table 6, Fig. 7).

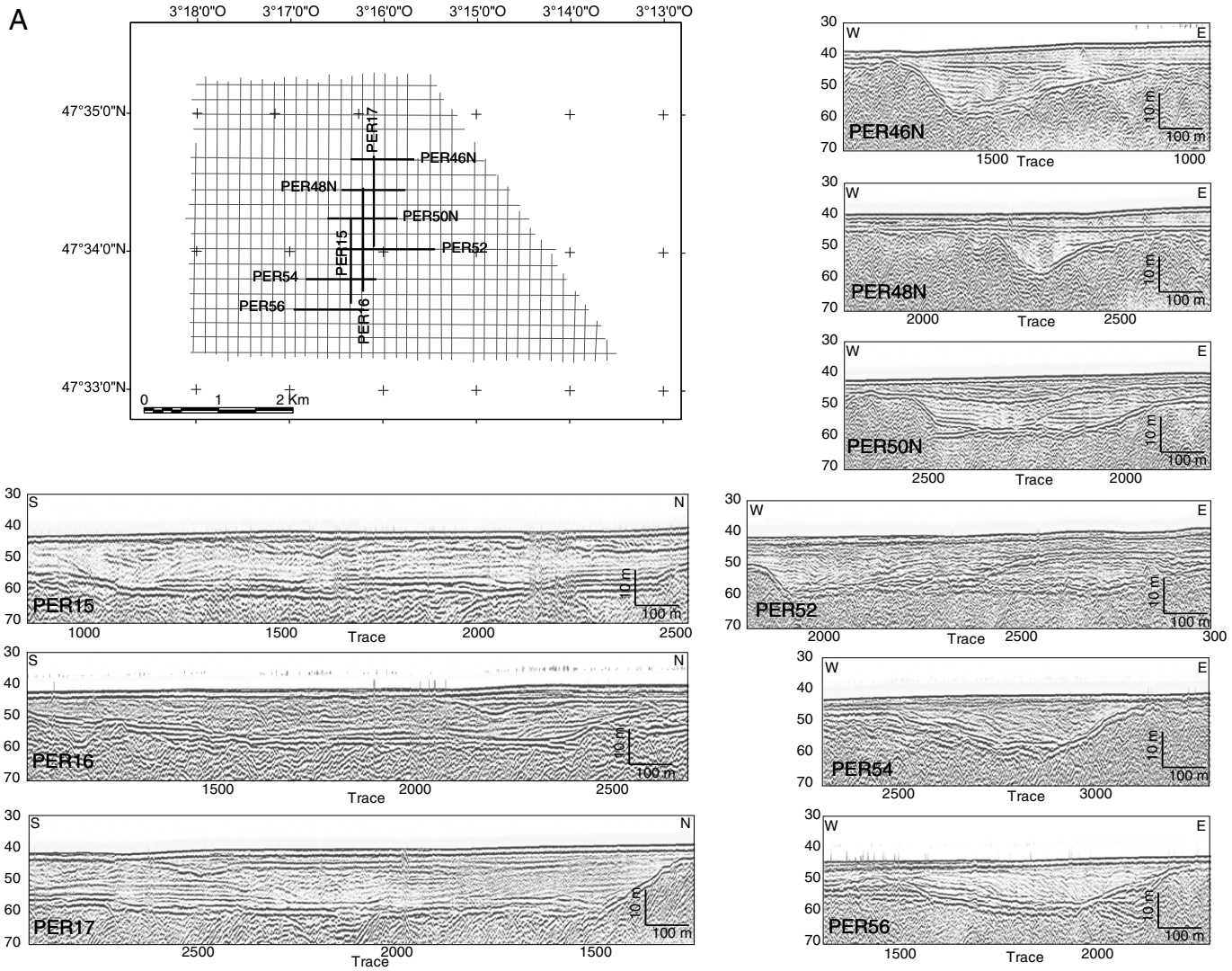


**Fig. 6.** A) Raw cross section along the paleo-valley. B) Interpreted cross sections showing the evolution of surfaces topographies along the paleo-valley. On profiles 46, 48 N and 50 N, the configuration of reflectors between S2 and S3 revealed the relics of an aggradating channel inside the sedimentary unit (U3). The channelized morphology of S3 lightly erodes the edges of this channel but re used this topography.

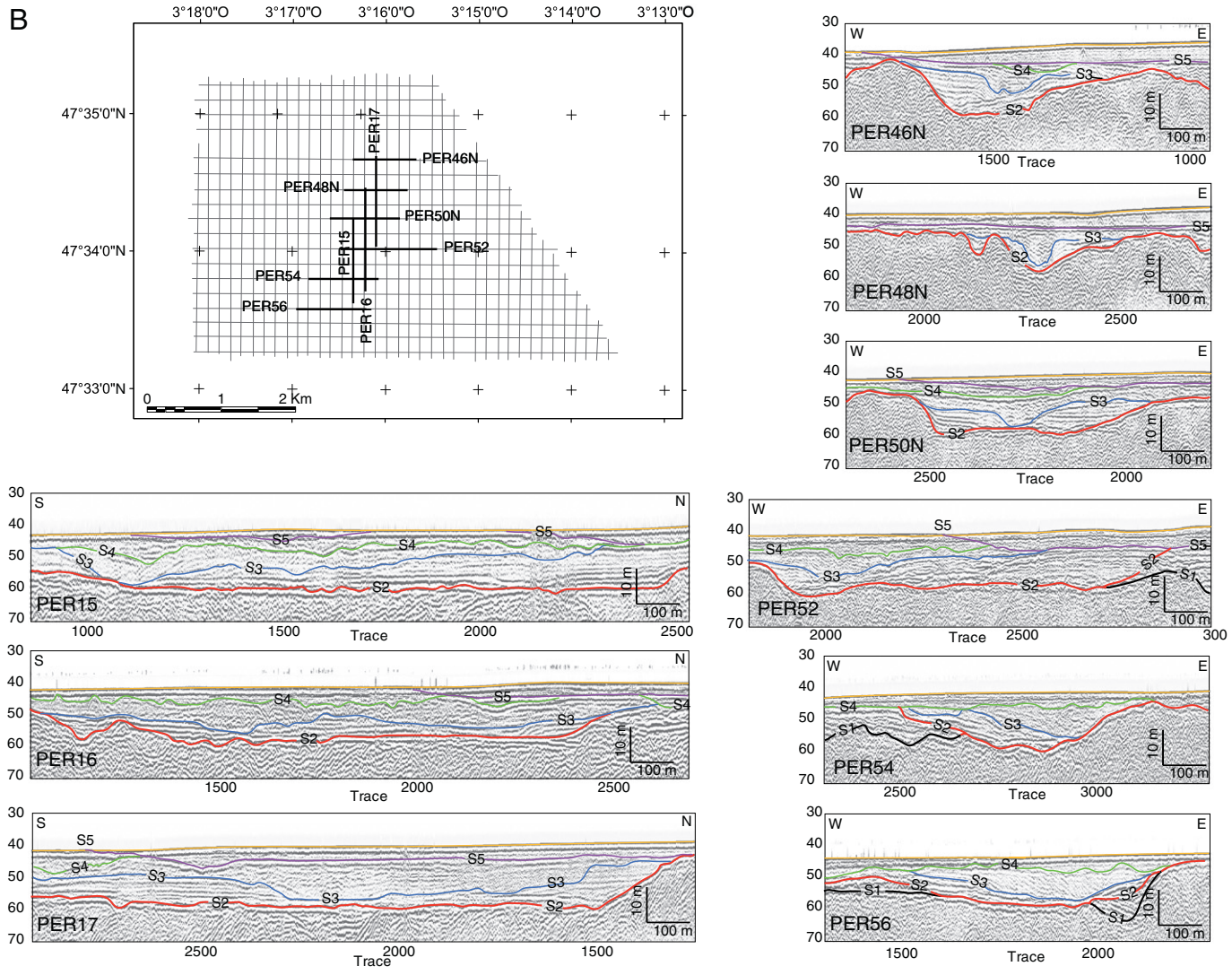


**Fig. 6** (*continued*).

## 5. Discussion

### *5.1. Sedimentary processes and stratigraphic significance of seismic units and their boundary surfaces*

Seismic unit and boundary surfaces of the study zone can be divided in two groups: (1) the basement made up of U1, S1 and U2 which are deformed and tilted; and (2) the overlying postglacial stacked soft sediments (between S2 and the present day sea floor) within and above of the channelized morphology of S2. The latter constitute the core of the new analysis of the current study.

#### *5.1.1. Surface S2*

Within the confines of the Bay of Etel, the dendritic organization of S2 channels (Figs. 1, 5A and 9A) suggests fluvial incision acquired during the exposure of the shelf during sea level lowstand. The paleo-hydrographic network presents a steep slope and high values of W/D ratio (Tables 2 and 3) within straight to sinuous channels (Fig. 5A). In modern fluvial classification, these geomorphological characteristics correspond to straight river systems involving bed-load transportation processes potentially forming braided deposits if the sediment load is sufficient (Schumm, 1985; Rosgen, 1994). Braided deposits are very sparse within ancient and modern Southern Brittany river systems and have not been recognized in the Etel System (Menier, 2004; Menier et al., 2006). It is often the case in the proximal part of fluvial systems, which would have been erosional, or have acted as a bypass zone (Zaitlin et al., 1994) instead of being a sedimentary accumulation zone. Additionally, the small drainage area of this river (600 km$^2$) limits the volume of sediment available for transport and preservation on the shelf of a large amount of sediments. In comparison, the Vilaine River system located a few kilometers south-eastwards of our study area, has a drainage area >10,000 km$^2$, and extensive coarse-grained lowstand deposits are widely recognized (Proust et al., 2001; Brault et al., 2004).

#### *5.1.2. Unit 3*

The first sedimentary sequence (seismic unit U3) is observed only within the paleo-Etel Channel (S2) fill (Fig. 9A, B). It contains horizontal highly reflective stratifications more common in fine grains deposits (mud and fine sand) than in coarser ones (coarse sand to pebble). Fine sediment aggradation is generally associated with low-energy environment, incompatible with fluvial deposition in a straight and steep-banked fluvial channel. The paleo-channel appears to be passively infilled with a suggestion of minor currents action, as marked by the presence of the internal aggrading channel within U3 (Figs. 6A, B and 9A, B). We then assume a transgressive origin for this unit and relate its deposition to the transgressive drowning of the fluvial channel S2. Such a depositional pattern is commonly encountered in tidal flat architecture: flood tides fill the estuary and allow the sedimentation

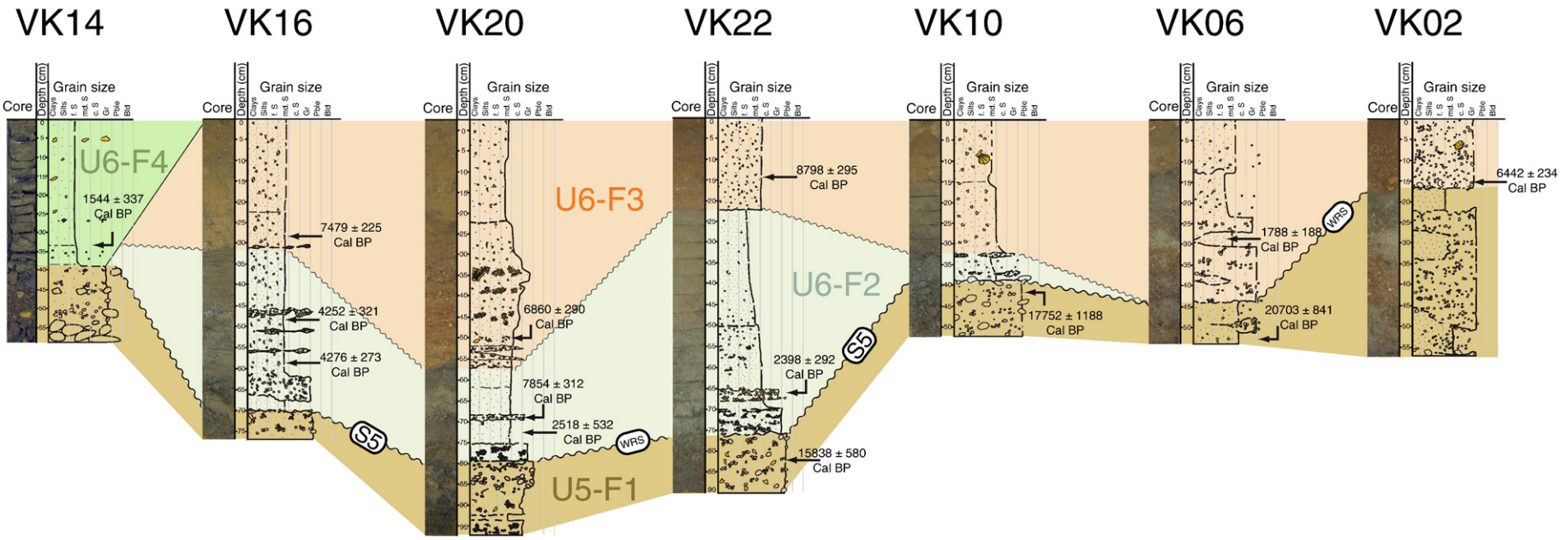


**Fig. 7.** Correlation of sedimentary facies in cores (see location in Fig. 2) and radiocarbon dating results locations. The top of U5 and the whole of U6 are visible on cores as wave ravinement surface S5. A later transgressive surface, not visible at seismic resolution, has been identified on cores between U6-F2 and U6-F3. Abbreviation: f.S. = fine sand; md.S. = medium sand; c.S. = coarse sand; Gr. = granule; Pble. = pebble; Bld. = boulder.

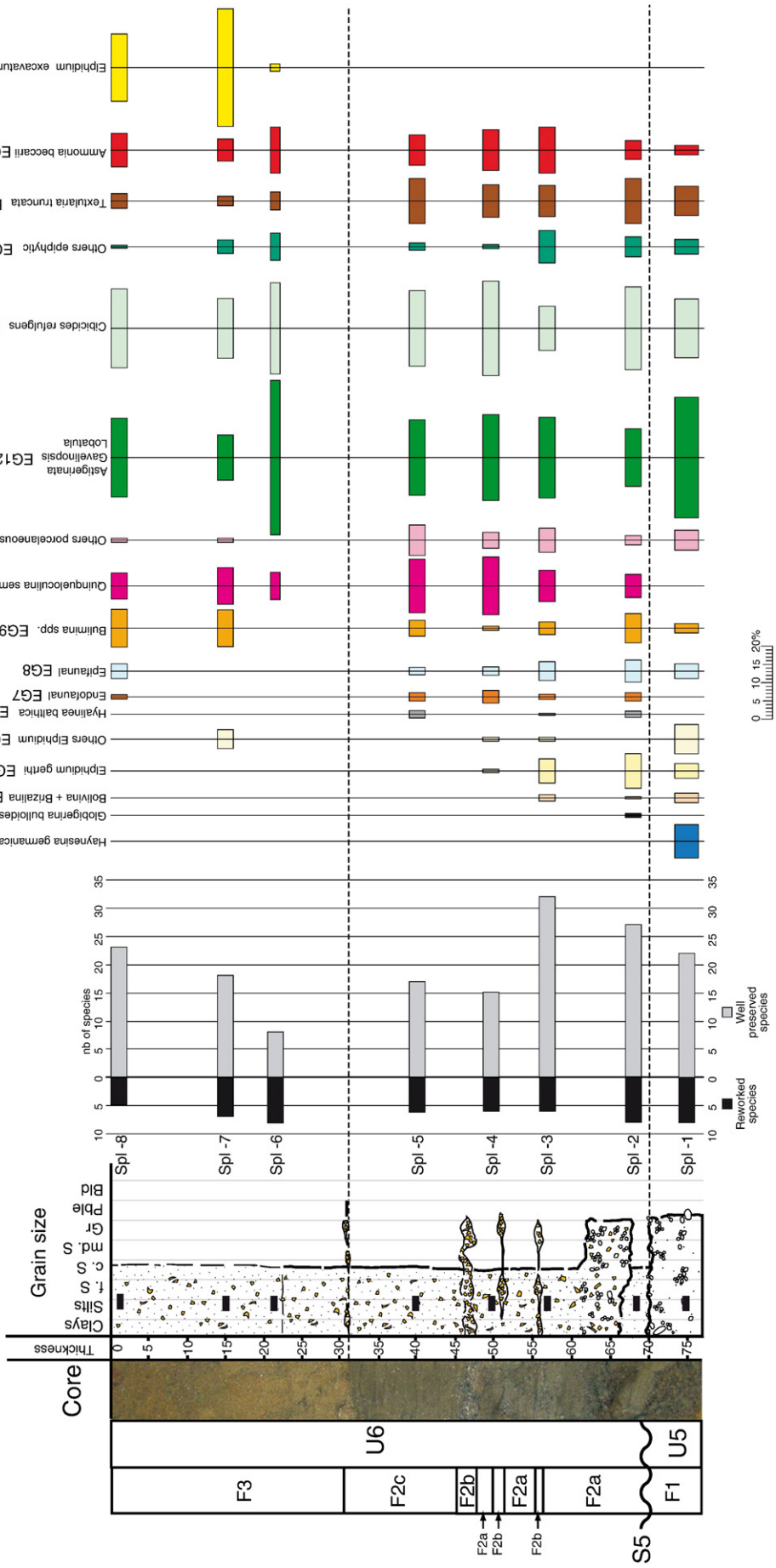


**Fig. 8.** Foraminiferal analysis in term of proportion and representation of the position of samples used for foraminiferal content analysis of core VK16.

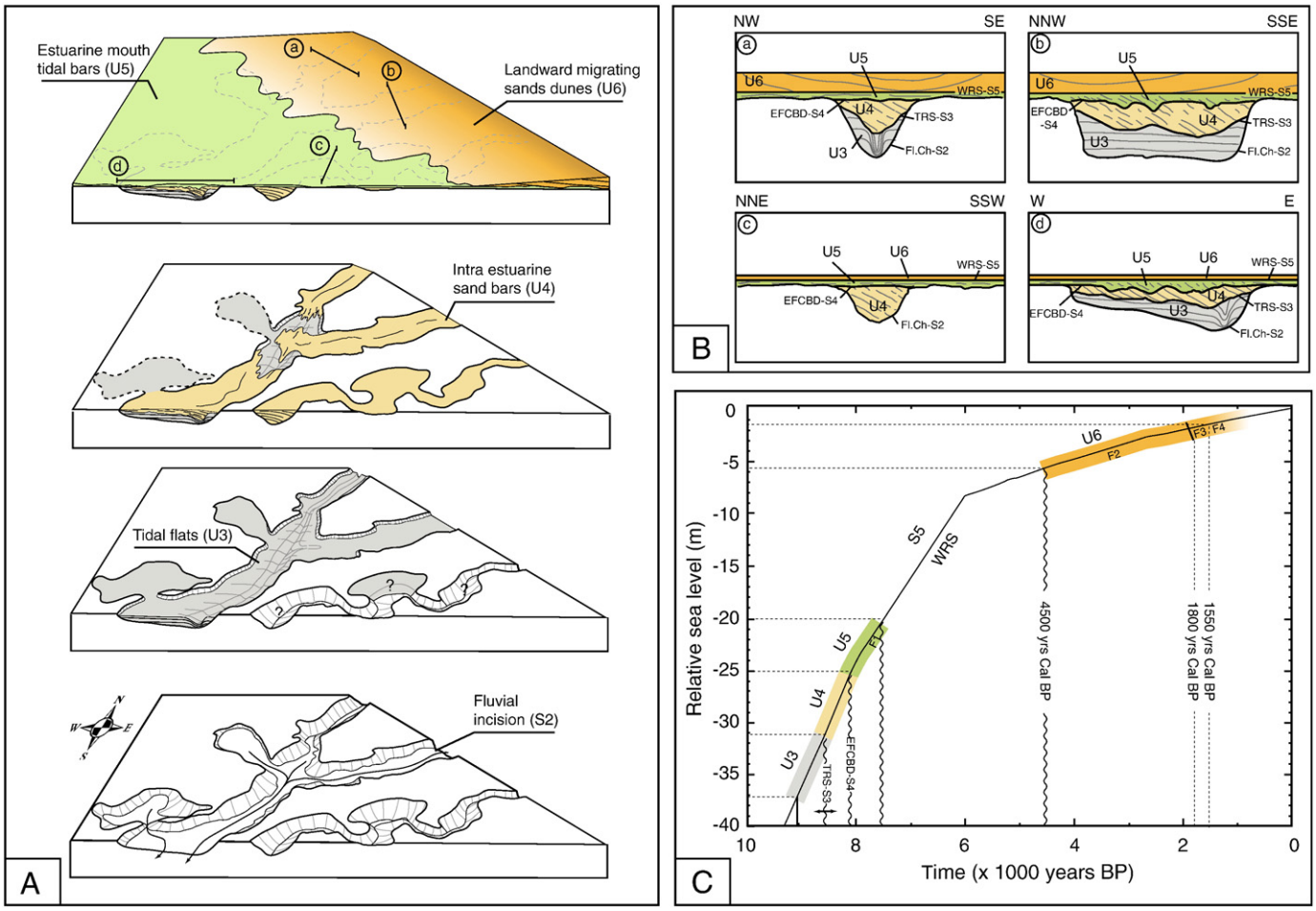


**Fig. 9.** Synthesis figure. A) Block diagrams presenting the stage of deposition on the study area. B) Schematic cross sections (location in Fig. 9A) showing the internal organization of the sedimentary filling in each sector of the drainage network. Fl.Ch: Fluvial Channel, TRS: Tidal Ravinement Surface, EFCBD: Ebb-Flood Channel Base Diastem, WRS: Wave Ravinement Surface. C) Position of seismic units and boundary surfaces on the relative sea-level curve proposed by Lambeck (1997) for Brittany coasts.

of fine particle while ebb tides drain the estuary and create a central drainage channel (Dalrymple and Choi, 2007). According to eustatic charts available on the Brittany coasts (Lambeck, 1997), the mean depth of S2 surface (−37 m LATL) is reached by mean sea level by around 9000 yr BP (Fig. 9C). This age marks the oldest sedimentary fill preserved in the paleo-Etel River as no lowstand deposits have been recognized.

*5.1.3. Surface S3*

The top of U3 is bounded by the erosional and channelized surface S3. The morphology of S3 can be interpreted as a second fluvial incision superimposed on the former S2 fluvial channel (Figs. 5A and 9B; Table 3). However, its complete confinement within S2 channels associated to its peculiar morphology of flat-dipping "pools" within the straight channel is not in agreement with such an interpretation. This erosional surface may correspond to the tidal ravinement surface (TRS) described by Allen and Posamentier (1993) as the interface between the estuarine tidal flats and the transgressive sandy tidal inlet. The scoured base results from tidal erosion in the narrow tidal inlet at the estuary mouth. Zaitlin et al. (1994) indicate that the TRS could effectively be mistaken with a fluvial incised surface (sequence boundary SB) due to its channelized morphology. According to these authors, the differences between the SB and the TRS are that (i) the second is confined within the first and that (ii) the TRS is highly local and cannot be correlated regionally, which is in good agreement with the situation of the paleo-Etel River.

*5.1.4. Unit 4*

Compared to U3, the seismic signature of this unit appears to be less reflective which may be the result of coarsening grain size. What is more, the presence of south-eastwards migrating clinoforms indicates a change in the depositional pattern passing from low-energy conditions and passive filling of the channel in U3 (interpreted as tidal flat), to subaquatic dynamic transportation of coarser particles. Nevertheless, this unit is still confined within a channelized morphology and fills the available space that remains in the original valley (S2) after the deposition of U3 and its subsequent tidal erosion by S3. These migrating coarse-sand bodies are interpreted as intra-estuarine sand bars (cf. Dalrymple et al., 1992; Dalrymple and Choi, 2007) and mark a retrogradation of the sedimentary environments passing from intertidal position with U3 to subtidal environments in U4.

*5.1.5. Surface S4*

This surface constitutes the interface between U4 and U5 forming a shallow and poorly defined channel that only reuses parts of the former flow directions (Fig. 9B). This surface is consistent with short interruptions or shifts in deposition (diastem) rather than with an uncorformity in the sense of Nummedal and Swift (1987) that involves a substantial break in the geological record. On the Virginia Shelf, Foyle and Oertel (1997) interpret these kinds of local scours as estuarine ebb-flood channel-base diastems (EFCBD) developed within the estuarine mouth sand complex and recording minor tidal scouring compared to TRS.

*5.1.6. Unit 5*

On seismic profiles, U4 and U5 appear to be quite similar in terms of depositional dynamic: both of them show reflections indicating an eastward progradation. However, U5 is the first unit that is not confined within the incisions initiated with the onset of S2. But paleo-topography still controls the location of S4 smooth channelized surface. U5 overflows the banks of the fluvial channels and is deposited as a thin sedimentary drape outside of it (Fig. 9A and B). The period of deposition no longer confined within the channel is assumed to coincide with the complete flooding of the shelf by the transgressing shoreline (Fig. 9C). Cores confirm the coarse grain size for U5 (Fig. 7). Deposition occurred in shallow water (equivalent to an estimated paleo-bathymetry comprised between −5 and −10 m) but the presence of *H. germanica* (Fig. 8, Table 5) indicates that this environment is still influenced by the inputs of fresh water marking the proximity of the land (cf. Section 4.2.1).

Shells dated in U5 between 20,700 and 15,800 cal yr BP have high values of $\delta^{13}C$ indicating a marine origin for these carbonated shells (Gupta and Polach, 1985) (Table 4, Fig. 7). Sea level is too low (ca. −120 m) at this period in the Bay of Etel to explain the presence of these marine shells (Lambeck, 1997) (Fig. 9C).

Ergo, dating results suggest that U5 incorporate alloctonous offshore elements imported in a brackish environment during the post glacial transgression indicating an intermediate position between estuarine and marine conditions. Similarly, paleontological considerations would suggest a deposition around 7500 yr BP (Fig. 9C). This environment could be interpreted as estuarine mouth tidal bars or ebb tidal delta deposits (Dalrymple and Choi, 2007) at the estuary mouth.

*5.1.7. Surface S5*

Contrarily to S3 and S4, the topography of S5 is characterized by the absence of channel incision (Figs. 5A and 9B). It erodes the top of the channel filling and laterally the alluvial plain. These data suggest a genetic disconnection with the morphology of S2 reflecting a change in dominant sedimentary process from localized erosion to regional development of a flat ravinement. Such an erosional surface is interpreted as the result of shoreface advance and wave abrasion action during sea level rise (Allen and Posamentier, 1993; Zaitlin et al., 1994) and marks the passage to purely marine environments.

*5.1.8. Unit 6*

The seismic records of U6 deposits shows tangential oblique reflectors that mark the landwards migration of sand banks (Figs. 4 and 6, Table 1). Cores reveal that the base of U6 is composed of a thin fine-grain horizon (F2), masked in seismic section by the immediately underlying high amplitude reflector of S5. This fine grains horizon is dated between 4250 and 2400 cal yr BP and is interpreted as deposited in a low-energy environment with paleo-bathymetry ranging from −10 to −20 m (Fig. 9C). It is interpreted to be a prodeltaic marine mud (F2a and F2c — Fig. 7), punctuated by storm deposits in F2b sedimentary facies. Sedimentary processes drastically change upwards with the deposition of the F3 sedimentary facies presenting highly reworked coarse-grained shoreface sands. This change in depositional conditions is also marked by a decrease of the foraminiferal diversity and by the incorporation of numerous allochthonous shell fragments. These poorly sorted sands are dated between the end of F2 (2400 cal yr BP) and 1800 cal yr BP which is the youngest age obtained from dated samples in F3 (Fig. 9C).

*5.2. Hypothesis about the onset of the basal channel surface S2*

In southern Brittany, the onset of the basal incision is poorly known due to a lack of dates in the sedimentary filling of the paleo-valleys.

Superficial samples of Late Oligocene sands in the Bay of Concarneau suggest that the Odet Quaternary fluvial system is superimposed on a former Oligocene incision (Delanoë et al., 1976). Nevertheless, the uncertain positioning of these samples makes this chronostratigraphical pattern quite hypothetical as there is no evidence of this type of deposits elsewhere on the shelf (Menier, 2004; Menier et al., 2006; Thinon et al., 2008).

Recent identification of Miocene sinuous fluvial incisions on the outer shelf (Paquet et al., 2010) poses a question about their connection with the Mio-Pliocene river systems identified by Guillocheau et al. (1998) on the Armorican Massif ashore. These discontinuous paleo-river networks (both incision and deposits) have been interpreted to be disconnected to the present-day drainage network in the emerged Armorican massif (Bonnet, 1998; Brault et al., 2004) and a priori offshore. The paleo-Etel River system appears to be the drowned extension of the present Etel River (Pinot, 1974; Vanney, 1977; Menier et al., 2006) invalidating a Miocene attribution. On the Armorican massif, the present day organization of the drainage system is assumed to be no older than 1 Myr according to the available dates and chronostratigraphical correlation attempts (Monnier et al., 1981; Van Vliet-Lanoë et al., 1997; Bonnet, 1998; Bonnet et al., 2000). Similarly, incision of the drowned paleo-Etel River is most probably coeval and related to this history. The geomorphological analysis of the paleo-Etel River indicates high W/D ratio associated with straight channels convenient with braided river regime. This kind of fluvial regime is generally associated to high water discharge commonly encountered in peri-glacial environments (Miall, 1996). Such a fluvial stream type is strongly modulated by climatic forcing. During Quaternary, Brittany encountered several periods of peri-glacial conditions due to its position at mid latitudes and on the southern boundary of the Fenno-Scandian ice-sheets. The attribution of the river incision based on fluvial channel geometry analysis to just one peculiar climatic event remains speculative. It has been associated with the Late Pleistocene lowering of the sea level on the French Atlantic coast as most of the sedimentary infill is dated to the Holocene (Allen and Posamentier, 1993; Lericolais et al., 2001). However, the lack of evidence of multiple incised fluvial systems from previous glacial cycles during the Pleistocene remains problematic.

Supporting dates are required to constrain the timing of shelf incision events. Monnier et al. (1981) attributes the upper terrace of the Vilaine River to an ante-Elsterian glacial period (Cromerian complex sensu lato) by comparison to similar pedogenetic horizons located in Northern Brittany. Electron Spin Resonance (EPR) dating methods have been employed in the paleo-Vilaine River (Van Vliet-Lanoë et al., 1997; Brault et al., 2004). Basal braided river deposits from this fluvial system are dated at 600,000 yr, consistent with the Cromerian attribution of the upstream dated terrace (Monnier et al., 1981). Gibbard and Lewin (2009) report that the climate alteration, which characterizes the "Middle Pleistocene Transition", played a key role in the onset of incision and enlargement of European major rivers.

The lengthening of the dominant Milankovich cyclicity rising from 41,000 to 100,000 yr notably marks this major climatic transition. It resulted in an intensification of climatic contrasts between glacial and interglacial periods since the MIS 16 (725 to 650 kyr) at mid latitudes (Head and Gibbard, 2005). This climatic alteration is associated to an increase of the amplitude of sea level fluctuations, falling below the bathymetric curve −120 m (Head and Gibbard, 2005). What is more, river incisions would have been favored by bedrock erodability increase: the bedrock has been strongly weakened by more intense peri-glacial conditions during glacial periods and fluctuations of river flow due to long-standing alteration of rain regimes (Gibbard and Lewin, 2009).

In the paleo-Etel River, fluvial sediments would then have been swept out as no coarse material has been recognized on seismic profiles. Such a fact is commonly observed in larger river systems, fluvial deposits being preserved very locally within incised valleys. That is the case for the paleo-Channel River where "*the deeps that can be seen in the present topography represent the partial removal of the alluvial infilling during the Late-glacial* […] *The removal of the alluvial sediment occurred through the action of marine currents as the sea reoccupied the Channel* (during last-glacial)" (Antoine et al., 2003).

Fluvial sediments have been partially swept away, forming a fine to coarse meter-thick sediment cover on the channel seafloor, or have been reworked in-situ by the combining action of Quaternary sea level oscillations, Holocene transgression and strong tidal dynamic (Reynaud et al., 2003). On the Southern Brittany shelf, swept away sediments could correspond to the accumulations of soft sediment on the south-western side of the island and shoal barrier that bounds the inner regions (Fig. 1). It forms a 5 to 15 m thick sediment bulge at the foot of the Groix Island, seawards turning into a discontinuous meter to infra-meter thick soft sand cover, widespread over the platform (Estournès, 2011).

Considering (i) the age reported in the Vilaine River studies which are contemporaneous to the Middle Pleistocene Transition and (ii) the climatic control on the paleo-Etel River stream type shown by geomorphological analysis which is consistent with landwards paleo-drainage system of southern Brittany (Bonnet, 1998), a middle Pleistocene origin for Southern Brittany incisions appears to be possible.

## 6. Conclusion

Beyond the local interest, this article proposes a time constrained high resolution 3D reconstitution of the organization of a tidal dominated filling emplaced within an incised valley. The sedimentary filling of the paleo-Etel River consists in the drowning of a sedimentary starved fluvial channel during the Holocene transgression. The sedimentary record shows two phase of filling: (i) the first phase consists in the retrogradation of tidal facies within this channel passing from tidal flat deposits (U3) to estuarine sand bars (U4) both separated by the onset of the Tidal Ravinement Surface (S3). This stage is assumed to start at ca. 9000 yr BP and finished at ca. 7500 yr BP considering the mean sea level position on available eustatic curves (Lambeck, 1997). The second phase is coeval with the total filling of the available space in the channel topography: since this moment (estimated around 7500 yr BP), the sedimentation is not channelized anymore and the sedimentation is dominated by open marine influences. In a first time, the area is still subdued to tidal processes (S4). Overlying sedimentary deposits are interpreted as brackish highly reworked sand bars belonging to the estuary mouth zone (U5-F1). The onset of the Wave Ravinement Surface (S5) marks the onset of open marine conditions after 4300 cal yr BP. Marine sedimentation began with a thin layer of marine sandy muds recording storms events between 4300 and 2500 ans cal yr (U6-F2) passing upwards to landwards migrating shoreface sand dunes, installed between 1800 and 1550 ans cal yr (U6-F3 and F4).

The age of the basal fluvial incision remains speculative in the paleo-Etel River system. The geomorphological analysis of the channel incision corresponds to a high energy bedload stream associated to high W/D ratios related to great variations in water discharge. In Southern Brittany, such a type of river type is dated in the Vilaine River and dated to 600 ka. We propose to link this incision phase to the Middle Pleistocene Transition which is already known to have initiated the incision and enlargement of Western European major rivers by changing in European climatic dynamic.

## Acknowledgments

This study has been funded by the Société Lafarge Granulats Ouest and by the Université de Bretagne-Sud, within the framework of the PERI-ARMOR project, (Chief scientist: Dr. David Menier). The authors would like to thank Alan Orpin and Philipp Gibbard for their constructive comments and kind advices that help to improve the earlier version of the manuscript. We also would like to thank the société Astérie for the acquisition of seismic data on behalf of the société Lafarge Granulats Ouest and the société GSM that kindly allow their publication.

## References

Allen, L., Posamentier, H., 1993. Sequence stratigraphy and facies model of an incised valley fill; the Gironde Estuary, France. Journal of Sedimentary Research 63 (3), 378–391.
Andreiff, P., Boillot, G., Gennesseaux, M., 1968. Préreconnaissance géologique du Sud du Massif armoricain: affleurements de dépôts aquitaniens. Comptes Rendus de l'Académie des Sciences — Series D — Sciences naturelles 266, 1220–1222.
Antoine, P., Coutard, J.-P., Gibbard, P., Hallegouet, B., Lautridou, J.-P., Ozouf, J.-C., 2003. The Pleistocene rivers of the English Channel region. Journal of Quaternary Science 18, 227–243.
Ashley, G.M., Sheridan, R.E., 1994. Depositional model for valley fills on a passive continental margin. In: Dalrymple, R.W. (Ed.), Incised-Valley Systems: Origins and Sedimentary Sequences: SEPM Special Publication, vol. 51, pp. 285–301.
Bernhard, J.M., 1986. Characteristic assemblages and morphologies of benthic foraminifera from anoxic, organic-rich deposits; Jurassic through Holocene. Journal of Foraminiferal Research 16 (3), 207–215.
Blum, M.D., Törnqvist, T.E., 2000. Fluvial responses to climate and sea-level change: a review and look forward. Sedimentology 47, 2–48.
Bonnet, S., 1998. Tectonique et dynamique du relief: le socle Armoricain au Pléistocène. PhD Thesis, Université de Rennes I — Géosciences Rennes, 352 pp.
Bonnet, S., Guillocheau, F., Brun, J.-P., Van Den Driessche, J., 2000. Large-scale relief development related to Quaternary tectonic uplift of a Proterozoic-Paleozoic basement: The Armorican Massif, NW France. Journal of Geophysical Research 105 (B8), 19,273–19,288.
Borne, V., Chevalier, M., 1986. Tectonique récente, effondrement et remplissages sédimentaires cenozoïques en domaine armoricain. Livret Guide Colloque du Comité Français de Stratigraphie, Nantes . 99 pp.
Bouysse, P., Horn, R., 1968. Nouvelles données sur la structure du plateau continental sud-Armoricain (France). Comptes Rendus de l'Académie des Sciences — Series D — sciences naturelles 267, 690–693.
Brault, N., Bourquin, S., Guillocheau, F., Dabard, M., Bonnet, S., Courville, P., Esteoule-Choux, J., Stepanoff, F., 2004. Mio-Pliocene to Pleistocene paleotopographic evolution of Brittany (France) from a sequence stratigraphic analysis: relative influence of tectonics and climate. Sedimentary Geology 163 (3–4), 175–210.
Broecker, W.S., Olson, E.A., 1961. Lamont radiocarbon measurements VIII. Radiocarbon 3, 176–204.
Caumon, G., Collon-Drouaillet, P., Carlier, Le, de Veslud, C., Viseur, S., Sausse, J., 2009. Surface-based 3D modeling of geological structures. Mathematical Geosciences 41 (8), 927–945.
Chassé, C., Glémarec, M., 1976. Atlas des fonds meubles du plateau continental du golfe de Gascogne: Cartes sédimentaires. ICA Brest 10.
Chaumillon, E., Weber, N., 2006. Spatial variability of modern incised valleys on the French Atlantic coast: comparison between the Charente and the Lay-Sèvre incised valleys. In: Dalrymple, R., Leckie, D., Tillman, R. (Eds.), Incised Valleys in Time and Space: SEPM Special Publication, vol. 85, pp. 57–85.
Chaumillon, E., Proust, J., Menier, D., Weber, N., 2008. Incised-valley morphologies and sedimentary-fills within the inner shelf of the Bay of Biscay (France): a synthesis. Journal of Marine Systems 72 (1–4), 383–396.
Dalrymple, R.W., Choi, K., 2007. Morphologic and facies trends through the fluvial–marine transition in tide-dominated depositional systems: a schematic framework for environmental and sequence-stratigraphic interpretation. Earth-Science Reviews 81 (3–4), 135–174.
Dalrymple, R.W., Zaitlin, B.A., Boyd, R., 1992. Estuarine facies models; conceptual basis and stratigraphic implications. Journal of Sedimentary Research 62, 1130–1146.
Delanoë, Y., Lehébel, L., Margerel, J., Pinot, J., 1975. La baie de Concarneau est un bassin tectonique dans lequel d'épais dépôts du Lutétien supérieur ont été conservés. Comptes Rendus de l'Académie des Sciences — Series D — Sciences Naturelles 281, 1947–1950.
Delanoë, Y., Margerel, J., Pinot, J., 1976. En baie de Concarneau, l'Oligocène marin est discordant sur un Eocène ondulé, faillé et érodé, l'Aquitanien a voilé l'ensemble après une nouvelle pénéplanation. Comptes Rendus de l'Académie des Sciences — Series D — Sciences Naturelles 282, 29–32.
Duleba, W., Debenay, J.P., Eichler, B.B., de Mahiques, M.M., 1999. Holocene environmental and water circulation changes: foraminifer morphogroups evidence in Flamengo Bay (SP, Brazil). Journal of Coastal Research 15 (2), 554–571.
Estournès, G., 2011. Architectures et facteurs de contrôle des bassins quaternaires immergés du précontinent armoricain - Exemples de la paléovallée d'Etel (Bretagne Sud) et du Bassin des Ecrehou (Golfe Normand Breton) -. PhD Thesis, Université de Bretagne Sud, 281 pp.
Fatela, F., 1995. Contribution des Foraminifères benthiques profonds à la reconstitution des paléoenvironnements du Quaternaire récent de la Marge Ouest Ibérique (Marge Nord Portugaise et Banc de Galice). PhD Thesis, Université de Bordeaux I, 281 pp.
Fatela, F., Taborda, R., 2002. Confidence limits of species proportions in microfossil assemblages. Marine Micropaleontology 45 (2), 169–174.
Féniès, H., Lericolais, G., 2005. Internal architecture of an incised valley-fill on a wave- and tide-dominated coast (the Leyre incised valley, Bay of Biscay, France). Comptes Rendus Geosciences 337 (14), 1257–1266.
Foyle, A.M., Oertel, G.F., 1997. Transgressive systems tract development and incised-valley fills within a Quaternary estuary–shelf system: Virginia inner shelf, USA. Marine Geology 137 (3–4), 227–249.
Gibbard, P., Lewin, J., 2009. River incision and terrace formation in the Late Cenozoic of Europe. Tectonophysics 474 (1–2), 41–55.
Goubert, E., 1997. Les *Elphidium excavatum* (TERQUEM), foraminifères benthiques, vivant en Baie de Vilaine (Bretagne, France) d'octobre 1992 à septembre 1996: morphologie, dynamique de population et relations avec l'environnement. Réflexions

sur l'approche méthodologique, la lignée évolutive et l'utilisation en paléoécologie. PhD Thesis, Université de Nantes. 186 pp.
Goubert, E., Néraudeau, D., Rouchy, J.M., Lacour, D., 2001. Foraminiferal record of environmental changes: Messinian of the Los Yesos area (Sorbas Basin, SE Spain). Palaeogeography, Palaeoclimatology, Palaeoecology 175 (1–4), 61–78.
Gros, Y., Limasset, O., 1984. La bretagne méridionale au Cénozoïque -Essai de reconstitution à partir de la bibliographie. Document du BRGM, 80 pp.
Guilcher, A., 1948. Le relief de la Bretagne méridionale de la baie de Douarnenez à la Vilaine. H. PhD Thesis, Paris, La Roche-sur-Yon, 682 pp.
Guillocheau, F., Bonnet, S., Bourquin, S., Dabard, M., Outin, J., Thomas, E., 1998. Mise en évidence d'un réseau de paléovallées ennoyées (paléorias) dans le Massif armoricain: une nouvelle interprétation des sables pliocènes armoricains. Comptes Rendus de l'Académie des Sciences — Series IIA — Earth and Planetary Science 327 (4), 237–243.
Guillocheau, F., Brault, N., Thomas, E., Barbarand, J., Bonnet, S., Bourquin, S., Estéoule-Choux, J., Guennoc, P., Menier, D., Néraudeau, D., Proust, J., Wyns, R., 2003. Histoire géologique du Massif Armoricain depuis 140 Ma (Crétacé à l'actuel) — Geological history of the Armorican massif since 140 Myr (Cretaceous–present day). Bulletin d'Information des Géologues du Bassin de Paris 40 (1), 13–28.
Gupta, S.K., Polach, H.A., 1985. Radiocarbon Dating Practices at ANU: Handbook. Radiocarbon Laboratory, Research School of Pacific Studies, Australian National University, Canberra.
Hardenbol, J., Thierry, J., Farley, M.B., Jacquin, T., De Graciansky, P.C., Vail, P.R., 1998. Mesozoic and Cenozoic sequence chronostratigraphic framework of European basins. et In: Graciansky, P.C., de Hardenbol, J., Jacquin, T., Vail, P.R. (Eds.), Mesozoic and Cenozoic Sequence Stratigraphy of European Basins: SEPM Special Publication, vol. 60, pp. 3–13.
Head, M.J., Gibbard, P.L., 2005. Early–Middle Pleistocene transitions: an overview and recommendation for the defining boundary. In: Head, M.J., Gibbard, P.L., London, G.S.O. (Eds.), Early–Middle Pleistocene Transitions: The Land–Ocean Evidence: Geological Society of London Special Publications, 247, pp. 1–18.
Hughen, K.A., Baillie, M.G.L., Bard, E., Beck, J.W., Bertrand, C.J.H., Blackwell, P.G., Buck, C.E., Burr, G.S., Cutler, K.B., Damon, P.E., Edwards, R.L., Fairbanks, R.G., Friedrich, M., Guilderson, T.P., Kromer, B., McCormac, G., Manning, S., Bronk Ramsey, C., Reimer, P.J., Reimer, R., Remmele, S., Southon, J.R., Stuiver, M., Talamo, S., Taylor, F.W., van der Plicht, J., Weyhenmeyer, C.E., 2004. Marine04 marine radiocarbon Ag calibration, 0–26 cal kyr BP. Radiocarbon 46 (3), 1059–1086.
Lambeck, K., 1997. Sea-level change along the French Atlantic and Channel coasts since the time of the Last Glacial Maximum. Palaeogeography, Palaeoclimatology, Palaeoecology 129 (1–2), 1–22.
Lazure, P., Salomon, J.-C., 1991. Coupled 2-D and 3-D modelling of coastal hydrodynamics. Oceanologica Acta 14 (2), 173–180.
Lericolais, G., Berné, S., Féniès, H., 2001. Seaward pinching out and internal stratigraphy of the Gironde incised valley on the shelf (Bay of Biscay). Marine Geology 175 (1–4), 183–197.
Menier, D., 2004. Morphologie et remplissage des vallées fossiles sud-armoricaines: apport de la stratigraphie sismique. PhD Thesis, Université de Rennes I — Géosciences Rennes, 202 pp.
Menier, D., Reynaud, J., Guillocheau, F., Guennoc, P., Bonnet, S., Tessier, B., Goubert, E., 2006. Basement control on shaping and infilling of valleys incised at the southern coast of Brittany, France. In: Dalrymple, R., Leckie, D., Tillman, R. (Eds.), Incised Valleys in Time and Space: SEPM Special Publication, vol. 85, pp. 37–55.
Menier, D., Tessier, B., Proust, J., Baltzer, A., Sorrel, P., Traini, C., 2010. The Holocene transgression as recorded by incised-valley infilling in a rocky coast context with low sediment supply (southern Brittany, western France). Bulletin de la Societe Geologique de France 181 (2), 115–128.
Miall, A.D., 1996. The Geology of Fluvial Deposits: Sedimentary Facies, Basin Analysis, and Petroleum Geology. Springer-Verlag, Berlin Heidelberg New York.
Mitchum, R.M., Vail, P., Sangree, J.B., 1977. Seismic stratigraphy and global changes of sea level, Part 6: stratigraphy interpretation of seismic reflection patterns in depositional sequences. AAPG Memoir 26, 117–133.
Monnier, J.-L., Jumel, G., Jumel, A., 1981. Le Paléolithique inférieur de la côte 42 à Saint-Malo-de-Phily (Ille-et-Vilaine). Stratigraphie et industrie. Bulletin de la Société préhistorique française 78 (10–12), 317–328.
Montadert, L., 1979. Rifting and subsidence of the northern continental margin of the Bay of Biscay. Initial Reports of the Deep Sea Drilling Project, Washington, pp. 1025–1060.
Murray, J.W., 2003. An illustrated guide to the benthic foraminifera of the Hebridean Shelf, west of Scotland, with notes on their mode of life. Palaeontologia Electronica 5 (1), 1–31.
Nafe, J.E., Drake, C.L., 1961. Physical Properties of Marine Sediments. Technical Report. Lamont Geological Observatory.
Nordfjord, S., Goff, J.A., Austin, J., Sommerfield, C.K., 2005. Seismic geomorphology of buried channel systems on the New Jersey outer shelf: assessing past environmental conditions. Marine Geology 214 (4), 339–364.
Nummedal, D., Swift, D.J.P., 1987. Transgressive stratigraphy at sequence-bounding unconformities: some principles derived from Holocene and Cretaceous examples. In: Nummedal, D., Pilkey, O.H., Howard, J.D. (Eds.), Sea-level Fluctuation and Coastal Evolution: SEPM Special Publication, vol. 41, pp. 241–260.
Olivet, J., 1996. La cinématique de la plaque Ibérique. Bulletin des Centres de Recherches, Exploration–Production Elf- Aquitaine 21, 131–195.
Paquet, F., Menier, D., Estournès, G., Bourillet, J., Leroy, P., Guillocheau, F., 2010. Buried fluvial incisions as a record of Middle–Late Miocene eustasy fall on the Armorican Shelf (Bay of Biscay, France). Marine Geology 268 (no. 1–4), 137–151.
Perez-Belmonte, L., 2008. Caractérisation environnementale, morphosédimentaire et stratigraphique du Golfe du Morbihan pendant l'Holocène terminal: implications évolutives. Université de Bretagne Sud.
Pinot, J., 1974. Le précontinent Breton entre Penmarc'h, Belle-île et l'escarpement continental, étude géomorphologique. PhD Thesis, Lannion, impram, 256 pp.
Polach, H., Gower, J., Fraser, I., 1973. Synthesis of high-purity benzene for radiocarbon dating. In: Rafter, T.A., Grant-Taylor, T. (Eds.), Proceedings of 8th International Conference on Radiocarbon Dating, Wellington, Royal Society of New Zealand, pp. B36–B49.
Preux, R., 1978. Rapport de fin de sondage Penma-1, Loire Maritime permit, S.N.E.A.P. (Société National Elf Aquitaine Production). BEPH (Bureau Exploration-Production des Hydrocarbures) Open File Report 14–3435. 15 pp.
Proust, J.-N., Menier, D., Guillocheau, F., Guennoc, P., Bonnet, S., Rouby, D., Le Corre, C., 2001. Les vallées fossiles de la baie de Vilaine: nature et évolution du prisme sédimentaire côtier du Pléistocène armoricain. Bulletin de la Société Géologique de France 172 (6), 737–749.
Redois, F., 1996. Les foraminifères benthiques actuels bioindicateurs du milieu marin exemples du plateau continental sénégalais et de l'estran du golfe du Morbihan (France). Université d'Angers.
Reynaud, J.-Y., Tessier, B., Auffret, J.-P., Berné, S., Batist, M.D., Marsset, T., Walker, P., 2003. The offshore Quaternary sediment bodies of the English Channel and its western approaches. Journal of Quaternary Science 18 (no.3-4), 361–371.
Rosgen, D.L., 1994. A classification of natural rivers. Catena 22 (3), 169–199.
Schumm, S.A., 1985. Patterns of Alluvial Rivers: Annual Review of Earth and Planetary Sciences 13, no. 1, pp. 5–27.
Schumm, S.A., 1993. River response to baselevel change: implications for sequence stratigraphy. Journal of Geology 101 (2), 279–294.
Severin, K.P., 1983. Test morphology of benthic foraminifera as a discriminator of biofacies. Marine Micropaleontology 8 (1), 65–76.
Shackleton, N., 1987. Oxygen isotopes, ice volume and sea level. Quaternary Science Reviews 6 (3–4), 183–190.
Sorrel, P., Tessier, B., Demory, F., Baltzer, A., Bouaouina, F., Proust, J., Menier, D., Traini, C., 2010. Sedimentary archives of the French Atlantic coast (inner Bay of Vilaine, south Brittany): depositional history and late Holocene climatic and environmental signals. Continental Shelf Research 30, 1250–1266.
Stuiver, M., Reimer, P.J., Reimer, R., 2005. CALIB 5.0.1. http://calib.org.
Tessier, C., 2006. Caractérisation et dynamique des turbidités en zone côtière: l'exemple de la région marine de Bretagne Sud, PhD thesis, Université de Bordeaux 1, 376 pp.
Thinon, I., Menier, D., Guennoc, P., Proust, J., 2008. Carte géologique de la France à 1/250 000 de la marge continentale (Feuille Lorient). Éditions BRGM-CNRS.
Toucanne, S., Zaragosi, S., Bourillet, J., Gibbard, P., Eynaud, F., Giraudeau, J., Turon, J., Cremer, M., Cortijo, E., Martinez, P., Rossignol, L., 2009. A 1.2 Ma record of glaciation and fluvial discharge from the West European Atlantic margin. Quaternary Science Reviews 28 (25–26), 2974–2981.
Vail, P., Mitchum, R.M., Thomson, I., 1977. Seismic stratigraphy and global changes of sea level, Part 4: global cycles of relative changes of sea level. AAPG Memoir (26), 83–97.
Van Vliet-Lanoë, B., Bonnet, S., Hallegouët, B., Laurent, M., 1997. Neotectonic and seismic activity in the Armorican and Cornubian Massifs: regional stress field with glacio-isostatic influence. Journal of Geodynamics 24 (1–4), 219–239.
Vanney, J., 1977. Géomorphologie de la marge continentale sud armoricaine. PhD Thesis, Université Paris-Sorbonne, 493 pp.
Zaitlin, B.A., Dalrymple, R.W., Boyd, R., 1994. The stratigraphic organization of incised valley systems associated with relative sea level change. In: Dalrymple, R.W. (Ed.), Incised-valley Systems: Origins and Sedimentary Sequences: SEPM Special Publication, vol. 51, pp. 45–60.